

# Functional Analysis of Lipid Metabolism in *Magnaporthe grisea* Reveals a Requirement for Peroxisomal Fatty Acid $\beta$ -Oxidation During Appressorium-Mediated Plant Infection

Zheng-Yi Wang, Darren M. Soanes, Michael J. Kershaw, and Nicholas J. Talbot

School of Biosciences, University of Exeter, Washington Singer Laboratories, Perry Road, Exeter, EX4 4QG, U.K.

Submitted 5 October 2006. Accepted 12 December 2006.

**The rice blast fungus *Magnaporthe grisea* infects plants by means of specialized infection structures known as appressoria. Turgor generated in the appressorium provides the invasive force that allows the fungus to breach the leaf cuticle with a narrow-penetration hypha gaining entry to the underlying epidermal cell. Appressorium maturation in *M. grisea* involves mass transfer of lipid bodies to the developing appressorium, coupled to autophagic cell death in the conidium and rapid lipolysis at the onset of appressorial turgor generation. Here, we report identification of the principal components of lipid metabolism in *M. grisea* based on genome sequence analysis. We show that deletion of any of the eight putative intracellular triacylglycerol lipase-encoding genes from the fungus is insufficient to prevent plant infection, highlighting the complexity and redundancy associated with appressorial lipolysis. In contrast, we demonstrate that a peroxisomally located multifunctional, fatty acid  $\beta$ -oxidation enzyme is critical to appressorium physiology, and blocking peroxisomal biogenesis prevents plant infection. Taken together, our results indicate that, although triacylglycerol breakdown in the appressorium involves the concerted action of several lipases, fatty acid metabolism and consequent generation of acetyl CoA are necessary for *M. grisea* to complete its prepene- tration phase of development and enter the host plant.**

*Additional keyword:* virulence.

Rice blast disease is a persistent threat to the global rice harvest, causing substantial crop losses every year (Talbot 2003). Rice blast infections are initiated by the spores of *Magnaporthe grisea*, an ascomycete fungus, which are spread by splash dispersal and adhere tightly to the hydrophobic rice leaf cuticle by means of an adhesive carried in the spore tip (Hamer et al. 1988). The spores quickly germinate and, within 8 h, each can form a specialized infection structure called an appressorium (Talbot 2003). The dome-shaped, single-celled appressorium attaches to the leaf surface with great force and develops substantial internal turgor, which is required for cuticle penetration (de Jong et al. 1997; Howard et al. 1991). Then, a narrow

penetration hypha is formed from the base of the cell and breaches the cuticle, becoming internalized within a host epidermal cell. Here, the fungus develops bulbous, branched invasive hyphae, which are bounded by the invaginated plasmalemma of the plant cell. After the initial asymptomatic phase, which lasts for up to 3 days, *M. grisea* causes large, necrotic disease lesions to form on rice leaves. In severe cases, the fungus can cause the whole seedling to die; whereas, in older plants, it can prevent grain filling or destroy the grain-bearing structures of the plant (Howard and Valent 1996; Talbot 2003).

To learn about the biology of plant infection by phytopathogenic fungi, we and others are studying the genetic regulation of appressorium development and turgor generation in *M. grisea* (Dean 1997; Talbot 2003; Wang et al. 2005). Appressorium formation is a widespread characteristic of crop pathogens and, therefore, represents a good stage in the life cycle for disease intervention. Durable control of rice blast disease has eluded both plant breeders and the developers of agrochemicals, and is an important long-term aim of our studies. The genetic tractability of *M. grisea*, coupled with access to its full genome sequence and that of its host, rice (Dean et al. 2005; Yu et al. 2002), provides an excellent opportunity for defining the principal determinants of appressorium-mediated plant infection and developing a more detailed understanding of the physiology of fungal infections of plants.

*M. grisea* appressoria are melanin-pigmented, dome-shaped cells and the only physical requirements to induce their formation are a hard, hydrophobic surface and the absence of external nutrients (Talbot 2003). This final point is very significant because it highlights the fact that the entire plant infection process from spore germination to development of the penetration hypha is fuelled by storage reserves carried in the spore. *M. grisea* conidia contain storage reserves in the form of trehalose, glycogen, and lipid bodies (Thines et al. 2000). Previous experiments have demonstrated that lipid bodies are mobilized quickly from the conidium to the germ tube apex and the incipient appressorium during development on the leaf surface. Subsequently, lipid bodies coalesce and, eventually, are taken up by vacuoles (Weber et al. 2001) in the appressorium. Meanwhile, the conidium collapses and undergoes programmed autophagic cell death, which is a prerequisite to appressorium maturation (Veneault-Fourrey et al. 2006). Appressoria contain high levels of triacylglycerol lipase activity during turgor generation, and very high concentrations of the compatible solute glycerol have been measured in appressoria (de Jong et al. 1997; Thines et al. 2000). Lipid body mobilization is regu-

Corresponding author: N. J. Talbot; E-mail: n.j.talbot@exeter.ac.uk

\*The e-Xtra logo stands for “electronic extra” and indicates the online version contains supplemental material not included in the print edition. Two tables, five figures, and additional information about methods are published online.

lated by the Pmk1 MAP kinase signaling pathway (Zhao et al. 2005) and the subsequent breakdown of lipids within the appressorium requires cAMP-dependent protein kinase A (Thines et al. 2000). A consequence of lipolysis in the appressorium is the generation of both fatty acids and glycerol. Therefore, a requirement for fatty acid  $\beta$ -oxidation and subsequent activation of the glyoxylate cycle and gluconeogenesis has been proposed (Thines et al. 2000; Weber et al. 2001). Consistent with this idea, the glyoxylate cycle was shown recently to be significant during plant infection by *M. grisea*. Mutants lacking the *ICL1* gene encoding isocitrate lyase show a delay in generation of disease symptoms (Wang et al. 2003). Interestingly, the glyoxylate cycle has been shown to be required for pathogenicity of other phytopathogenic and human pathogenic fungi (Idnurm and Howlett 2002; Lorenz and Fink 2001; Solomon et al. 2004), perhaps reflecting their shared need to develop initially within a glucose-deficient environment. The fact that *Δicl1* mutants still were able to cause rice blast symptoms, however, suggested that alternative metabolic pathways are likely to be necessary for appressorium maturation and penetration hypha development (Bhambra et al. 2006; Wang et al. 2005).

$\beta$ -Oxidation is the principal means by which fatty acids are metabolized in cells. The mechanism of  $\beta$ -oxidation involves a set of four consecutive reactions catalyzed by four major enzymes in the process of fatty acid oxidation: acyl-CoA oxidase, 2-enoyl-CoA hydratase, 3-hydroxacyl-CoA dehydrogenase, and 3-ketoacyl-CoA thiolase. Through this four-step pathway, a two-carbon unit is split from each fatty acid in the form of an acetyl-CoA unit, which then can be fed in to the glyoxylate cycle or degraded in the citric acid cycle to produce  $\text{CO}_2$  and  $\text{H}_2\text{O}$ . There are several other enzymatic activities, such as *cis*-enoyl-CoA isomerase, which also are necessary for the degradation of unsaturated fatty acids. Multifunctional proteins (MFPs) include at least two of these enzymatic activities, 2-enoyl-CoA hydratase and 3-hydroxacyl-CoA dehydrogenase, which are involved in the second and third steps of the fatty acid  $\beta$ -oxidation cycle. Both mitochondrial and peroxisomal  $\beta$ -oxidation occur in mammals; whereas, in yeasts and plants,  $\beta$ -oxidation appears to be restricted to peroxisomes, which harbor the full enzymatic machinery to degrade fatty acids (Ecker and Erdmann 2003; Hiltunen et al. 2003; Van Roermund et al. 2003). Recently, it has been found that both mitochondrial and peroxisomal  $\beta$ -oxidation occur in the filamentous fungus *Aspergillus nidulans* (Maggio-Hall and Keller 2004). The role of triacylglycerol breakdown and fatty acid  $\beta$ -oxidation in appressorium function of *M. grisea* has not yet been studied and is the subject of this report.

To determine the role of triacylglycerol metabolism, fatty acid  $\beta$ -oxidation, and peroxisomal biogenesis in appressorium mediated plant infection by *M. grisea*, we utilized the genome

sequence of the fungus (Dean et al. 2005) to identify all of the genes that potentially are involved in lipolysis and fatty acid metabolism. We then systematically tested the role of a subset of these genes in appressorium function by targeted gene deletion to determine the relative importance of triacylglycerol breakdown and subsequent fatty acid  $\beta$ -oxidation to appressorium physiology. Our study has highlighted the extensive redundancy in fungal triacylglycerol lipases and the critical role that peroxisomal fatty acid  $\beta$ -oxidation plays in the early stages of plant infection by the rice blast fungus.

## RESULTS

### Genomic analysis of the genes involved in lipolysis and fatty acid $\beta$ -oxidation of *M. grisea*.

Rapid mobilization of lipid bodies takes place during infection-related development in *M. grisea* and is followed by breakdown of triacylglycerol (TAG), when appressoria mature and develop turgor (Thines et al. 2000). Lipid bodies are broken down to generate fatty acids and glycerol by the action of TAG lipases; therefore, we set out to identify the inventory of lipases and esterases encoded within the *M. grisea* genome. Putative intracellular lipase-encoding genes, which represent the most likely candidates for playing a role in lipid body breakdown, are listed in Table 1. Seven lipase-encoding genes were predicted to encode intracellular enzymes. Two *M. grisea* loci showed high levels of similarity to *TGL1* and one locus to the *TGL2* intracellular TAG lipase-encoding genes from *Saccharomyces cerevisiae*. Tgl1 originally was classified as a triglyceride-specific lipase, but recent evidence indicates that it acts as a membrane-anchored steryl esterase (Köffel et al. 2005). Tgl2, meanwhile, has lipolytic activity and may be required for degradation of diacylglycerol, although there is no detectable phenotype associated with *Δtgl2* mutants (Van Heusden et al. 1998). Two *M. grisea* genes were very similar to mammalian hormone-sensitive lipases, involved in TAG mobilization (Harbitz et al. 1999), and two loci showed high levels of identity to the Tgl3 lipid particle-associated TAG lipase which is required for intracellular lipolysis of lipid bodies in *S. cerevisiae* (Athenstaedt and Daum 2003). To investigate TAG lipase gene expression, RNA gel blots were prepared from *M. grisea* mycelium that had been grown in the presence of glucose, acetate, olive oil, the triglyceride triolein, and oleic acid as sole carbon sources (Fig. 1). RNA also was extracted from germinating spores prior to appressorium development. Elevated expression of *TGL1-2*, *TGL3-2*, and *HDL2* was observed in the presence of olive oil as a sole carbon source. *TGL1-1* was induced in expression in minimal medium and by acetate, olive oil, and oleic acid, and two of the lipase genes, *HDL1* and *TGL1-2*, were highly expressed in conidia of *M. grisea*, consistent with a role in lipid mobilization. Expression levels

**Table 1.** Genes predicted to encode intracellular triacylglycerol lipases in the genome of *Magnaporthe grisea*

Gene	Predicted open reading frame	Top nonhypothetical hit vs. NCBI nr <sup>a</sup>	Predicted location <sup>b</sup>	Pfam motifs <sup>c</sup>
HDL1	MG02376.4	Hormone-sensitive lipase, <i>Sus scrofa</i> (4e-14)	Nuclear	...
HDL2	MG10755.4	Lipase, <i>Bacillus cereus</i> (2e-37)	Cytoplasmic	...
TGL1-1	MG02622.4	Triglyceride lipase-cholesterol esterase, <i>Schizosaccharomyces pombe</i> (1e-106)	Cytoplasmic	$\alpha/\beta$ Hydrolase fold, ab-hydrolase associated lipase region
TGL1-2	MG00528.4	Steryl ester hydrolase; Yeh2p, <i>Saccharomyces cerevisiae</i> (2e-57)	ER	...
TGL2	MG00773.4	Triglyceride lipase; Tgl2p, <i>Saccharomyces cerevisiae</i> (3e-35)	Mitochondrial	...
TGL3-1	MG05933.4	Lipid particle protein; Ste1p, <i>Saccharomyces cerevisiae</i> (1e-102)	Nuclear	Patatin-like phospholipase
TGL3-2	MG09880.4	Tgl3 protein, <i>Kluveromyces delphensis</i> (2e-40)	ER	Patatin-like phospholipase

<sup>a</sup> BlastP used to compare predicted protein sequence against National Center for Biotechnology Information (NCBI) nonredundant database. Hits against hypothetical and putative proteins were discarded. E value of top hit in parentheses.

<sup>b</sup> Subcellular location of enzyme predicted using PSORT II. ER = endoplasmic reticulum.

<sup>c</sup> Protein family motifs for each predicted protein obtained from Broad Institute.

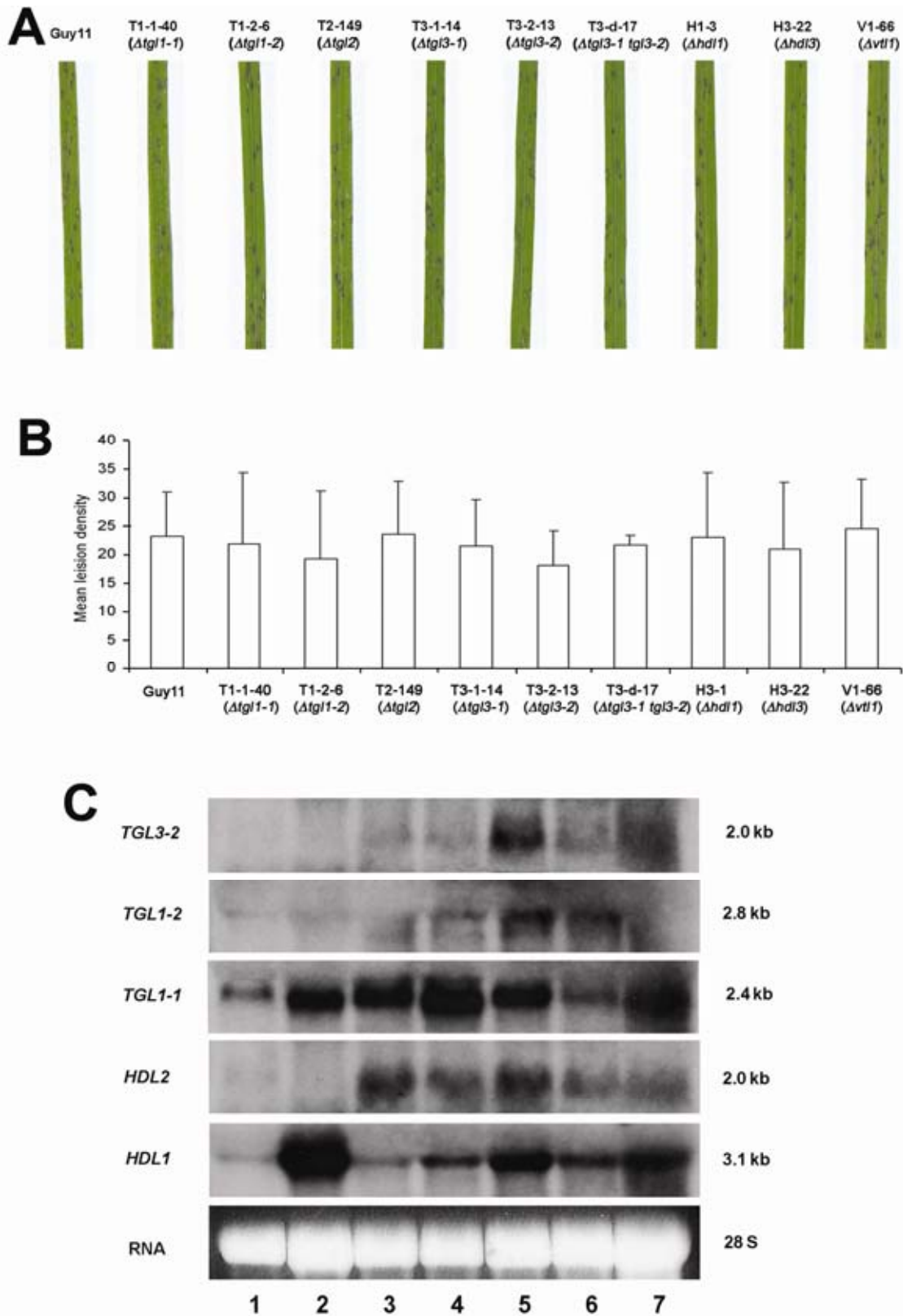


**Fig. 1.** Functional characterization of eight genes putatively encoding intracellular triacylglycerol lipases from *Magnaporthe grisea*. **A**, Rice leaves from seedlings of cv. CO-39 inoculated with a suspension of the wild-type *M. grisea* strain Guy11 and isogenic lipase gene replacement mutants at  $1 \times 10^4$  conidia  $\text{ml}^{-1}$ . T1-1-40:  $\Delta tgl1-1::Hph$  gene deletion mutant. T1-2-6:  $\Delta tgl1-2::Hph$ . T2-149:  $\Delta tgl2::Hph$ . T3-1-14:  $\Delta tgl3-1::Hph$ . T3-2-13:  $\Delta tgl3-2::Hph$ . T3-1/2-17:  $\Delta tgl3-1::Hph::\Delta tgl3-2::ilv$  double mutant. V1-66:  $\Delta vtl1::Hph$ . H1-3:  $\Delta hdl1::Hph$ . H3-22:  $\Delta hdl3::Hph$ . **B**, Bar chart showing quantitative analysis of rice infection assays. Mean lesion density values recorded from 5-cm section of the 15 most-infected leaves. The experiment was repeated three times. Error bars represent the standard deviation. **C**, RNA gel blot analysis of putative triacylglycerol lipase genes. Total RNA was extracted from lane 1, *M. grisea* mycelium grown in complete medium broth for 24 h; lane 2, *M. grisea* conidia; lane 3, *M. grisea* mycelium grown in minimal medium (MM) with glucose as sole carbon source for 24 h; lane 4, *M. grisea* mycelium grown in MM with sodium acetate as sole carbon source; lane 5, *M. grisea* mycelium grown in MM with olive oil; lane 6, *M. grisea* mycelium grown in MM with triolein; lane 7, *M. grisea* mycelium grown in MM with oleic acid. Restriction fragments from the coding regions of each lipase gene were used as the hybridization probes.

of *TGL2*, *TGL3-1*, *HDL3*, and *VTL1* were very low in all conditions tested (data not shown). Significantly, *M. grisea* also possesses 21 further lipase or carboxylesterase-encoding genes in its genome (Table 2). This includes a set of three genes, which show the highest similarity to previously characterized fungal extracellular lipases (Fickers et al. 2005; Nagao et al. 1994). Based on our genomic analysis, it seems likely that *M. grisea* possesses a significant battery of lipases, not only for secretion and degradation of substrates containing lipid but also for utilization of intracellular lipid bodies.

### Deletion of individual triacylglycerol lipases genes of *M. grisea* does not significantly affect fungal virulence.

To determine the role of the predicted intracellular TAG lipases on virulence of *M. grisea*, we generated targeted gene deletion mutants for eight of the *M. grisea* TAG lipase-encoding gene loci: *TGL1-1*, *TGL1-2*, *TGL2*, *TGL3-1*, *TGL3-2*, *HDL1*, *HDL3*, and *VTL1* (Tables 1 and 2). The candidates were chosen based on their predicted intracellular location or similarity to enzymes known to play a role in lipid mobilization. We also generated a *Δtgl3-1 Δtgl3-2* double mutant, based on the observation that these genes showed the greatest levels of identity to genes encoding lipid body-associated lipases from *S. cerevisiae* (Athenstaudt and Daum 2003). The strategies for the construction of gene-replacement vectors and identification of gene-replacement mutants are described in the Supplementary Methods available online and are shown in Supplementary Figure 1. We were unable to obtain a targeted deletion of *HDL2* despite screening in excess of 200 transformants. Rice plant infection assays showed that mutants *Δtgl1-1*, *Δtgl1-2*, *Δtgl2*, *Δtgl3-1*, *Δtgl3-2*, *Δhdl1*, *Δhdl3*, and *Δvtl1* and double mutant *Δtgl3-1 Δtgl3-2* all were able to cause rice blast disease and produced disease symptoms that were similar to the wild-type *M. grisea* strain Guy11 (Fig. 1). In addition, all mutants grew normally when supplied with olive oil, triolein, or oleic acid as sole carbon source (data not shown). These results suggested that no single TAG lipase was essential for fungal virulence and that none of the putative intracellular lipases is required for lipid substrate utilization. We conclude that intracellular lipolysis during appressorium morpho-

genesis involves either further, as yet unidentified, lipases or, more likely, the concerted action of a significant number of the TAG lipases that we identified by genome analysis.

### Fatty acid β-oxidation in the rice blast fungus.

A consequence of TAG lipase activity within the appressorium is a need for subsequent metabolism of the fatty acids generated. Comparative genomic analysis of the inventory of genes encoding enzymes involved in fatty acid β-oxidation in *M. grisea* and other fungal species therefore was carried out (Table 3). The budding yeast *S. cerevisiae* performs β-oxidation solely in peroxisomes. The first step is catalyzed by acyl-CoA oxidase, in which electrons are passed directly to molecular oxygen to form hydrogen peroxide. The next two reactions are catalyzed by a multifunctional β-oxidation protein. In mitochondrial β-oxidation, the first step is catalyzed by acyl-CoA dehydrogenase and electrons are passed to FAD to produce FADH<sub>2</sub>, which is passed to the electron transport chain. Enzymes catalyzing the other reactions are not part of a multifunctional β-oxidation protein but are separate entities. Analysis of the *M. grisea* genome indicates that it possesses a distinct pathway, which also is conserved in the related filamentous fungus *Neurospora crassa*, using acyl-CoA dehydrogenases (five in each case, presumably to deal with a wide range of substrates) but also having a multifunctional β-oxidation protein. Therefore, *M. grisea* and *N. crassa* both may be able to oxidize a wider range of substrates than *S. cerevisiae*, which can oxidize only straight chain fatty acids (hence the large number of acyl-CoA dehydrogenases in the filamentous fungi—one of which may be an isovaleryl CoA dehydrogenase in *M. grisea*). Consistent with this idea, *M. grisea* and *N. crassa* both have a homologue of α-methylacyl-CoA racemase, which is involved in the oxidation of branched chain amino acids (Table 3).

In order to investigate the role of fatty acid β-oxidation in appressorium physiology, a gene putatively encoding the multifunctional β-oxidation protein (MG06148.4) was isolated and named *MFP1*. The open reading frame (ORF) of *MFP1* was a 3,092-bp sequence including four introns, capable of encoding an 896-amino-acid (aa) protein. The putative gene product of

**Table 2.** Genes predicted to encode extracellular lipases or esterases in the genome of *Magnaporthe grisea*

Predicted ORF <sup>a</sup>	Top nonhypothetical hit vs. NCBI nr <sup>b</sup>	Predicted location <sup>c</sup>	Pfam motif <sup>d</sup>
MG07016.4	Extracellular lipase, <i>Gibberella zeae</i> (5e-83)	Extracellular	Lipase
MG09839.4	Extracellular lipase, <i>G. zeae</i> (9e-44)	Extracellular	Lipase
MG04555.4	Triacylglycerol lipase, <i>Candida deffmans</i> (5e-39)	Extracellular	Lipase
MG00314.4	Lipase, <i>Botryotinia fuckeliana</i> (0)	Extracellular	Carboxylesterases
MG02130.4	Carotenoid ester lipase, <i>Pleurotus sapidus</i> (5e-72)	Extracellular	Carboxylesterases
MG00499.4	Esterase EstA, <i>Aspergillus niger</i> (1e-129)	Endoplasmic reticulum	Carboxylesterases
MG08417.4	Acetylcholinesterase, <i>Mus musculus</i> (5e-44)	Extracellular	Carboxylesterases
MG08416.4	Esterase EstA, <i>A. niger</i> (7e-70)	Extracellular	Carboxylesterases
MG10414.4 (VTL1)	Esterase EstA, <i>A. niger</i> (1e-111)	Extracellular	Carboxylesterases
MG00440.4	Cephalosporin esterase, <i>Rhodospiridium toruloides</i> (2e-59)	Extracellular	Carboxylesterases
MG02497.4	Esterase EstA, <i>A. niger</i> (1e-41)	Plasma membrane	Carboxylesterases
MG09668.4	Cholinesterase 1, <i>Branchiostoma floridae</i> (2e-36)	Extracellular	Carboxylesterases
MG02827.4	Esterase EstA, <i>A. niger</i> (5e-44)	Extracellular	Carboxylesterases
MG04419.4	Cephalosporin esterase, <i>Rhodospiridium toruloides</i> (3e-41)	Extracellular	Carboxylesterases
MG02987.4	Carboxylesterase type B, <i>Novosporingobium aromaticivorans</i> (3e-37)	Extracellular	Carboxylesterases
MG08915.4	Carboxylesterase, <i>Athalia rosae</i> (4e-30)	Mitochondrial	Carboxylesterases
MG08468.4	Acetylcholinesterase, <i>Rattus norvegicus</i> (3e-30)	Extracellular	Carboxylesterases
MG10663.4	Carotenoid ester lipase, <i>Pleurotus sapidus</i> (6e-24)	Extracellular	Carboxylesterases
MG03772.4	Carboxyl ester lipase, <i>Gallus gallus</i> (4e-35)	Extracellular	Carboxylesterases
MG00593.4	Cholesterol esterase, <i>Rattus norvegicus</i> (2e-36)	Extracellular	Carboxylesterases
MG02521.4	Carboxylesterase, type B, <i>Deinococcus radiodurans</i> (3e-29)	Mitochondrial	Carboxylesterases

<sup>a</sup> ORF = open reading frame.

<sup>b</sup> BlastP used to compare predicted protein sequence against National Center for Biotechnology Information (NCBI) nonredundant database. Hits against hypothetical and putative proteins were discarded. E value of top hit in parentheses.

<sup>c</sup> Subcellular location of enzyme predicted using PSORT II.

<sup>d</sup> Protein family motifs for each predicted protein obtained from Broad Institute.

*MFPI* showed 80% amino acid identity to fox-2 from *N. crassa* (CAA56355) and 47% identity to fox-2 from *S. cerevisiae* (CAA82079).

### Fatty acid $\beta$ -oxidation is required for appressorium function in *M. grisea*.

To determine the role of fatty acid  $\beta$ -oxidation in pathogenesis of *M. grisea*, we characterized *MFPI* using a gene replacement strategy (Fig. 2A). Two transformants, MBO-7 and MBO-9, that had undergone the *MFPI* gene replacement (Fig. 2B) were identified and selected for further study. The  $\Delta mfp1$  mutants were unable to grow on olive oil, triolein, or oleic acid as sole carbon sources, consistent with an inability to metabolize fatty acids (Supplemental Figure 2). To investigate the role of *MFPI* in rice blast disease, conidial suspensions were sprayed onto seedlings of the susceptible rice cv. CO-39. A consistent reduction in disease lesion development was observed in plants inoculated with  $\Delta mfp1$  mutants (Fig. 2C and D). However, the virulence of  $\Delta mfp1$  mutants could be partially restored by addition of glucose (1 or 2.5%) to conidia prior to rice inoculation (Fig. 2E). Introduction of the *MFPI* gene into  $\Delta mfp1$  mutant MBO-7 completely restored its ability to cause disease and to utilize a range of lipid substrates (Supplementary Figure 3).

To determine when *MFPI* is expressed, RNA gel blot experiments were carried out in which RNA was isolated from *M. grisea* conidia, mycelium prepared in either rich growth medium or defined minimal medium with glucose, sodium acetate, olive oil, triolein, or oleic acid as sole carbon source (Fig. 3). *MFPI* was much more highly expressed in conidia than in vegetative mycelium and strongly induced by growth on lipids or fatty acids. *MFPI* also was induced in sodium acetate minimal medium, although at lower levels (Fig. 3A). In order to investigate the temporal and spatial pattern of *MFPI* expression during infection-related development, a 1.5-kb promoter fragment upstream of the gene and the entire *MFPI* protein-coding sequence were fused in-frame to the green fluorescent protein (GFP)-encoding gene *sGFP*. The *MFPI:sGFP* plasmid was introduced into a  $\Delta mfp1$  mutant, MBO-7, and transformants carrying a single integration of the plasmid were selected by DNA gel blot analysis (not shown). Two independent single insertion transformants, MBO-G-10 and MBO-G-19, were found to complement all

the  $\Delta mfp1$  mutant phenotype and, therefore, were used to investigate gene expression patterns and the localization of the protein. High levels of *MFPI:sGFP* fluorescence were found in conidia and in mycelium grown in the presence of olive oil (Fig. 3B), consistent with expression patterns revealed by RNA gel blot analysis. To determine the localization of Mfp1, we carried out colocalization studies with the foxA-red fluorescent protein (RFP) gene fusion (Maggio-Hall and Keller 2004). FoxA is a peroxisomally localized  $\beta$ -oxidation enzyme from *A. nidulans*, which contains a peroxisomal targeting signal 1 (PTS1) peroxisomal targeting sequence (Maggio-Hall and Keller 2004). Two single-copy plasmid insert transformants, MBO-G-R-21 and MBO-G-R-31, were identified and showed GFP and red fluorescent protein (RFP) fluorescence in a punctate distribution at exactly the same localization (Fig. 4). The results indicate that *M. grisea* Mfp1 is located in peroxisome-like bodies, which were often at the periphery of cells. We conclude that Mfp1 encodes a peroxisomally localized  $\beta$ -oxidation multifunctional protein required for lipid utilization and for fungal virulence.

### MgPex6-mediated peroxisome biogenesis is essential for appressorium-mediated plant infection by *M. grisea*.

Analysis of Mfp1 suggested that peroxisomal fatty acid  $\beta$ -oxidation is significant for appressorium-mediated plant infection by *M. grisea*. To test this hypothesis directly, we decided to generate a strain of the fungus in which peroxisomal biogenesis was impaired. We identified *MgPEX6*, which has a 4,310-bp coding sequence, including two introns, capable of encoding a 1,375-aa protein (MG00529.4). The putative gene product of *MgPEX6* is a peroxin protein essential for peroxisome biogenesis in eukaryotic cells and showed 60% identity to *ClAPEX6* from *Colletotrichum lagenarium* (AAK16738) and 38% identity to the *PAS8* peroxin gene from *S. cerevisiae* (CAA96261). Targeted deletion of *MgPEX6* was carried out and two independent  $\Delta mgpex6$  mutants, PEX-17 and PEX-26, were identified (Fig. 5). Neither of the  $\Delta mgpex6$  mutants of *M. grisea* could use olive oil, triolein, or oleic acid as a sole carbon source. We investigated the role of *MgPEX6* in growth, development, and virulence of *M. grisea*.  $\Delta mgpex6$  mutants did not form as many aerial hyphae as Guy11 and showed lighter colony pigmentation. Sporulation also was dramatically reduced; Guy11 produced a mean of  $138.33 \pm 24.13 \times 10^5$  co-

**Table 3.** Genes predicted to encode enzymes involved in fatty acid  $\beta$ -oxidation in genome of *Magnaporthe grisea*

Enzyme	Predicted ORF <sup>a</sup>	EC number <sup>b</sup>	Function	Predicted location <sup>c</sup>
Acyl-CoA-binding protein	MG06177.4		Intracellular carrier of acyl-CoA esters	Cytoplasmic
Long-chain fatty acyl-CoA ligase	MG01551.4	6.2.1.3	Activation of long-chain fatty acids	ER
Long-chain fatty acyl-CoA ligase	MG04956.4	6.2.1.3	Activation of long-chain fatty acids	Cytoplasmic
Long-chain fatty acyl-CoA ligase	MG07197.4	6.2.1.3	Activation of long-chain fatty acids	Cytoplasmic
Very-long-chain fatty acyl-CoA ligase	MG08257.4	6.2.1.3	Activation of very-long-chain fatty acids	Cytoplasmic
Acyl-CoA dehydrogenase	MG03418.4	1.3.99.-	Catalyzes first step in fatty acid $\beta$ -oxidation	Cytoplasmic
Acyl-CoA dehydrogenase	MG05949.4	1.3.99.-	Catalyzes first step in fatty acid $\beta$ -oxidation	Cytoplasmic
Acyl-CoA dehydrogenase	MG08661.4	1.3.99.-	Catalyzes first step in fatty acid $\beta$ -oxidation	Peroxisomal
Acyl-CoA dehydrogenase, short- or branched-chain specific	MG08690.4	1.3.99.2	Catalyzes first step in fatty acid $\beta$ -oxidation	Mitochondrial
Acyl-CoA dehydrogenase	MG10518.4	1.3.99.-	Catalyzes first step in fatty acid $\beta$ -oxidation	Peroxisomal
Multifunctional $\beta$ -oxidation protein	MG06148.4	4.2.1.-	Trifunctional hydratase-dehydrogenase-epimerase,	
		1.1.1.-	catalyzes second and third steps in fatty acid $\beta$ -oxidation	Cytoplasmic
$\beta$ -Ketoacyl-CoA thiolase	MG10700.4	2.3.1.16	Catalyzes final step in fatty acid $\beta$ -oxidation	Cytoplasmic
Short-chain enoyl-CoA hydratase	MG06272.4	4.2.1.17	Catalyzes second step in fatty acid $\beta$ -oxidation	Mitochondrial
delta3,delta2-Enoyl-CoA isomerase	MG00359.4	5.3.3.8	$\beta$ -Oxidation of unsaturated fatty acids	Mitochondrial
2,4-Dienoyl-CoA reductase	MG05138.4	1.3.1.34	$\beta$ -Oxidation of unsaturated fatty acids	Peroxisomal
delta 3,5-delta 2,4-Dienoyl-CoA isomerase	MG07309.4	5.3.3.-	Fatty acid $\beta$ -oxidation, auxiliary isomerization steps	ER

<sup>a</sup> ORF = open reading frame.

<sup>b</sup> - indicates that these enzymes do not fall neatly into the bottom level categories and are therefore only categorized to the third level.

<sup>c</sup> Subcellular location of enzyme predicted using PSORT II. ER = endoplasmic reticulum.

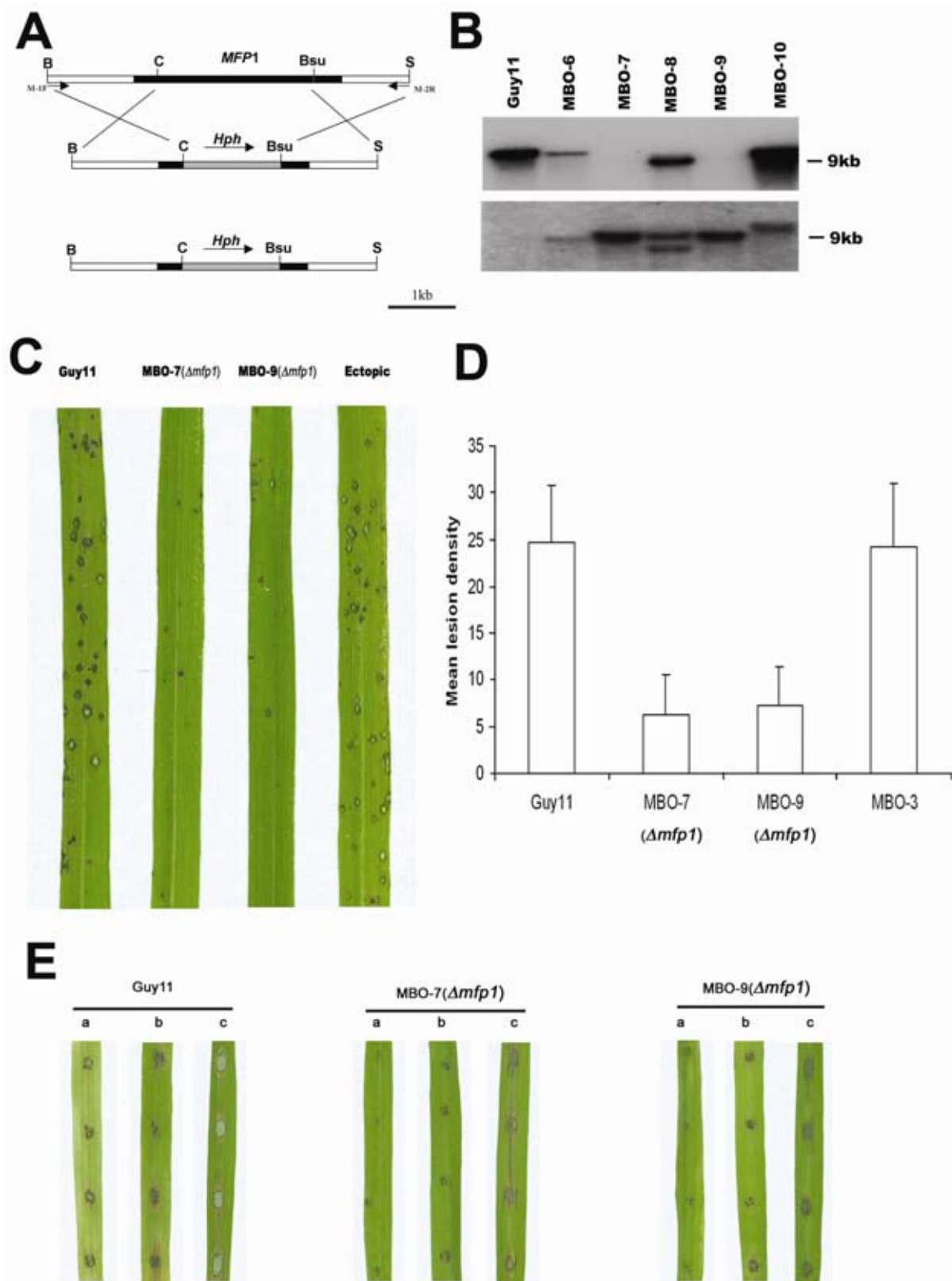


**Fig. 2.** *Magnaporthe grisea* *MFP1* gene is required for normal rice blast disease symptoms. **A.** *MFP1* gene replacement vector was constructed by amplifying a fragment spanning the *MFP1* locus with primers M-1F and M-2R, digesting the resulting amplicons with *Cla*I and *Bsu*36I, and ligating these to the *Hph* hygromycin phosphotransferase gene cassette. Restriction enzyme sites are *Bam*HI (B), *Cla*I (C), *Bsu*36I (Bsu), and *Spe*I (S). *Bam*HI and *Spe*I were introduced during the cloning process. **B.** DNA gel blot analyses of the wild-type strain (Guy11), two  $\Delta mfp1::Hph$  mutants (MBO-7 and MBO-9), and three ectopic transformants (MBO-6, MBO-8, and MBO-10). Genomic DNA samples were digested with *Eco*RI and probed with the removed *Cla*I/*Bsu*36I fragment (top) and the 1.4-kb *Hph* gene (bottom). **C.** Leaves of 14-day old-rice seedlings of cv. CO-39 were sprayed with conidia of Guy11, MBO-7( $\Delta mfp1$ ), MBO-9( $\Delta mfp1$ ), and an ectopic transformant (MBO-6) at a concentration  $1 \times 10^4$  conidia  $ml^{-1}$ . **D.** Bar chart showing the results of quantitative analysis of rice infection assays. Mean lesion density values recorded from 5-cm sections from 15 of the most infected leaves. Error bars represent the standard deviation. **E.** Rice leaf segments were inoculated with the conidial drops at a concentration  $1 \times 10^4$  conidia  $ml^{-1}$  from Guy11, MBO-7 ( $\Delta mfp1$ ), and MBO-9 ( $\Delta mfp1$ ); a = unwounded leaf, b = addition of 2.5% glucose to conidial suspension, and c = abraded leaf.

nidia per 10-day-old complete medium plate culture compared with  $3.16 \pm 2.65 \times 10^5$  for *Δmgpex6* strain PEX-17 and  $3.09 \pm 1.54 \times 10^5$  for PEX-26, after 12 days. Interestingly, the percentage of nonviable conidia of PEX-26 also dramatically increased as the age of the fungal mycelium increased (Supplementary Figure 4). Appressorium formation occurred at a slightly reduced frequency and most appressoria formed by PEX-26 were abnormal, small, and less melanized than those of Guy11. No disease lesions were observed in rice plants inoculated with *Δmgpex6* (Fig. 5C and D), indicating that perox-

isome function is necessary for plant infection by *M. grisea*. Virulence of *Δmgpex6* mutants could, however, be partially restored by addition of glucose (1 and 2.5%) to conidia prior to inoculation (Fig. 5E). *MgPEX6* also was required for growth of *M. grisea* in plant tissue because inoculation of wounded leaves, in which the cuticle was removed by abrasion, by *Δmgpex6* mutants did not result in rice blast symptoms (Fig. 5E). Introduction of the *MgPEX6* gene into *Δmgpex6* mutant PEX-26 restored its ability to grow on lipids and cause rice blast disease.

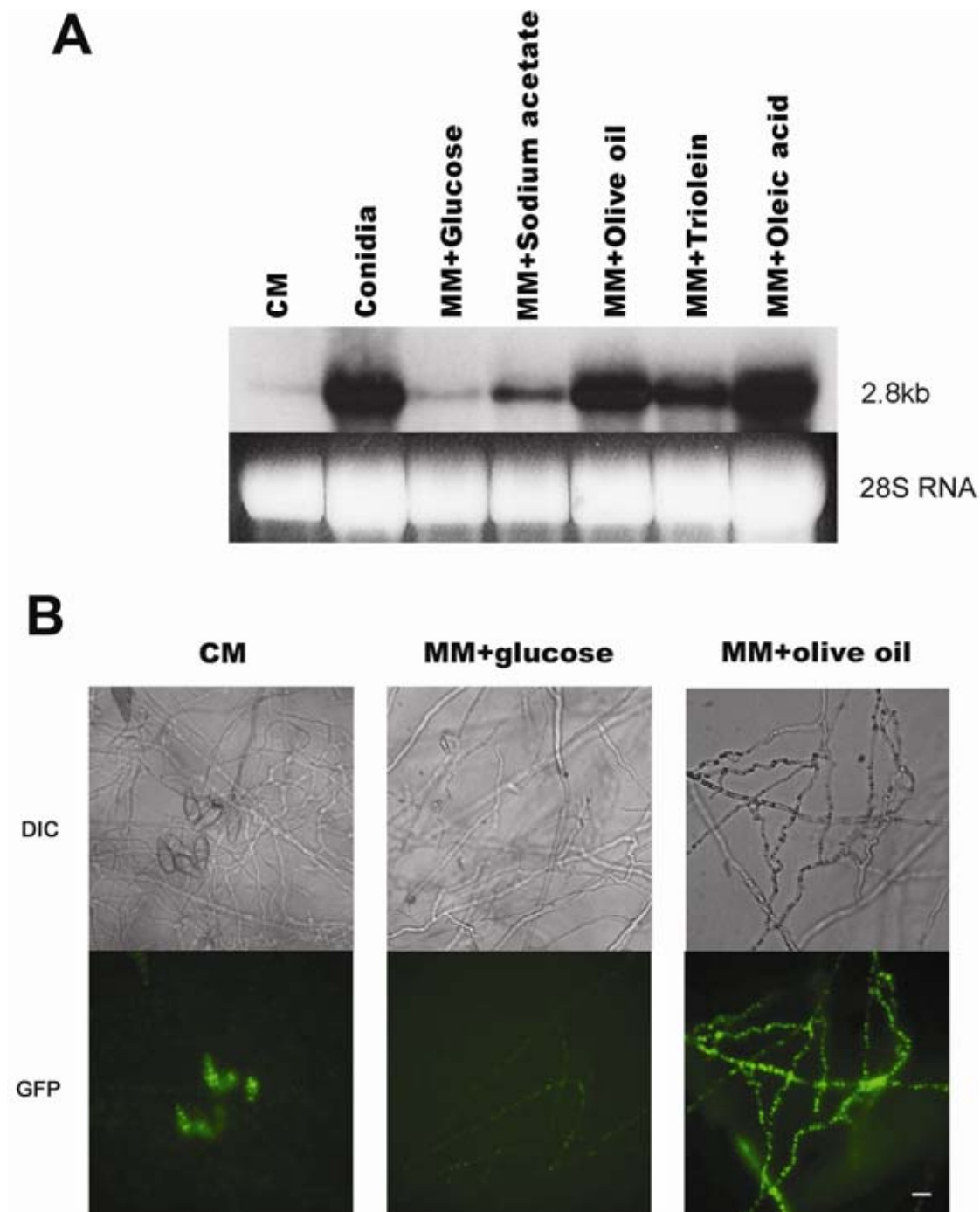


**Fig. 3.** Gene expression analysis of *Magnaporthe grisea* *MFPI*. **A**, RNA gel blot analysis of *M. grisea* *MFPI*. Total RNA was extracted from *M. grisea* mycelium grown in complete medium (CM) broth, *M. grisea* conidia, and mycelium grown in minimal medium (MM) with glucose, sodium acetate, olive oil, triolein, or oleic acid as sole carbon source. The blot was hybridized with a *ClaI/Bsu36I* fragment of the *MFPI* coding region. **B**, Spatial analysis of *MFPI* gene expression in response to the presence of lipid. A transformant of MBO-7 was selected (M-green fluorescent protein [GFP]-10) expressing an *MFPI-sGFP* gene fusion. The level of Mfp1-GFP fluorescence was observed in conidia (left), and in hyphae induced exposed to glucose (middle) or olive oil (right) as sole carbon sources. All GFP images were taken with identical exposure time. Bar for all frames = 10  $\mu$ m.

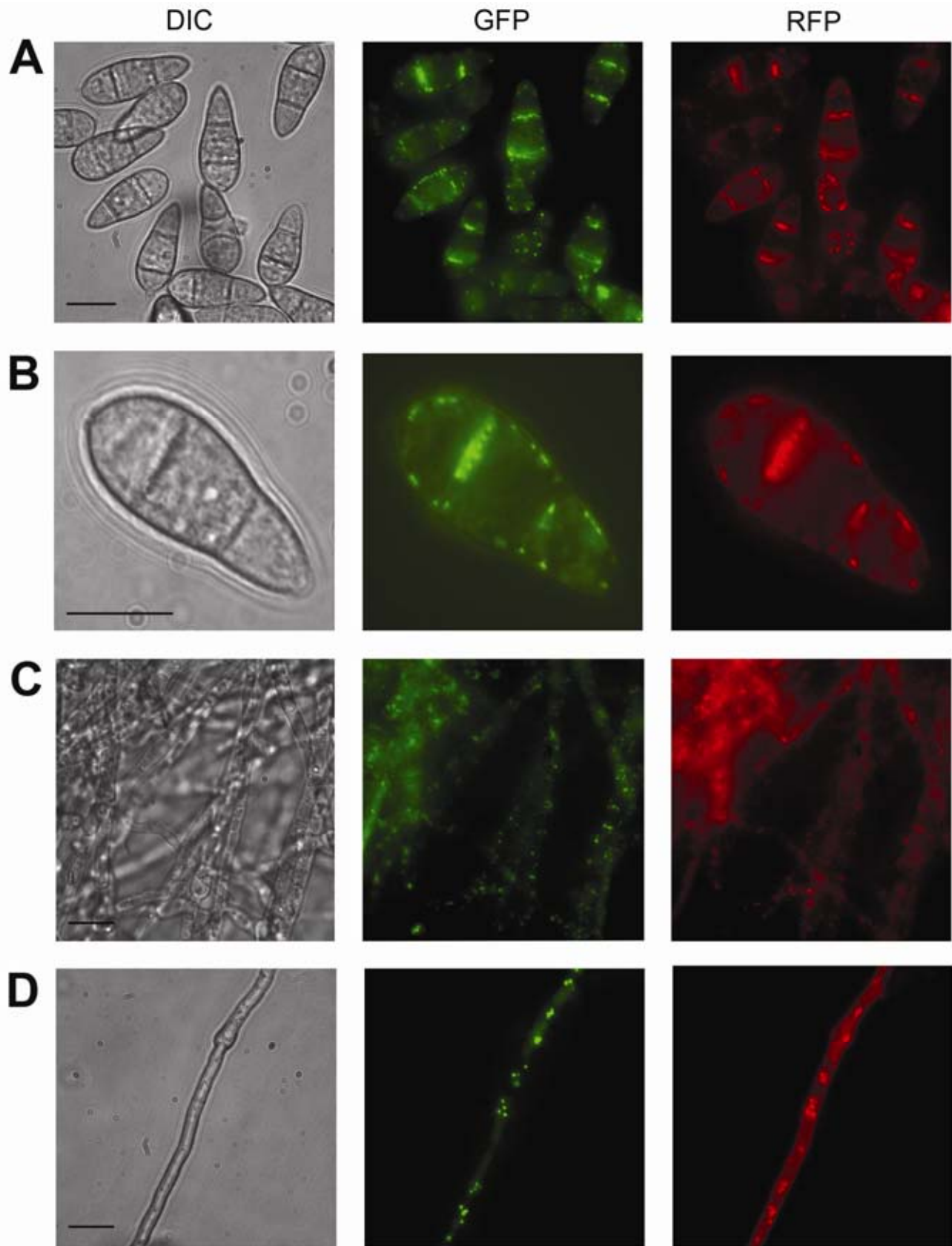


**Fig. 4.** Intracellular localization of Mfp1-s-green fluorescent protein (GFP) and colocalization with foxA-red fluorescent protein (RFP). Mycelium and conidia of a transformant expressing *MFPI-sGFP* and *foxA-RFP* were observed by epifluorescence microscopy. DIC = differential interference contrast. **A** and **B**, Conidia were harvested from 10-day-old complete medium agar plates and GFP and RFP fluorescence were observed in a punctate pattern consistent with peroxisomal localization. Peroxisomes were observed more frequently at the periphery of conidia rather than in the central region. **C** and **D**, Mycelium was incubated in complete medium for 48 h before observation. Bar for all frames = 10  $\mu$ m.

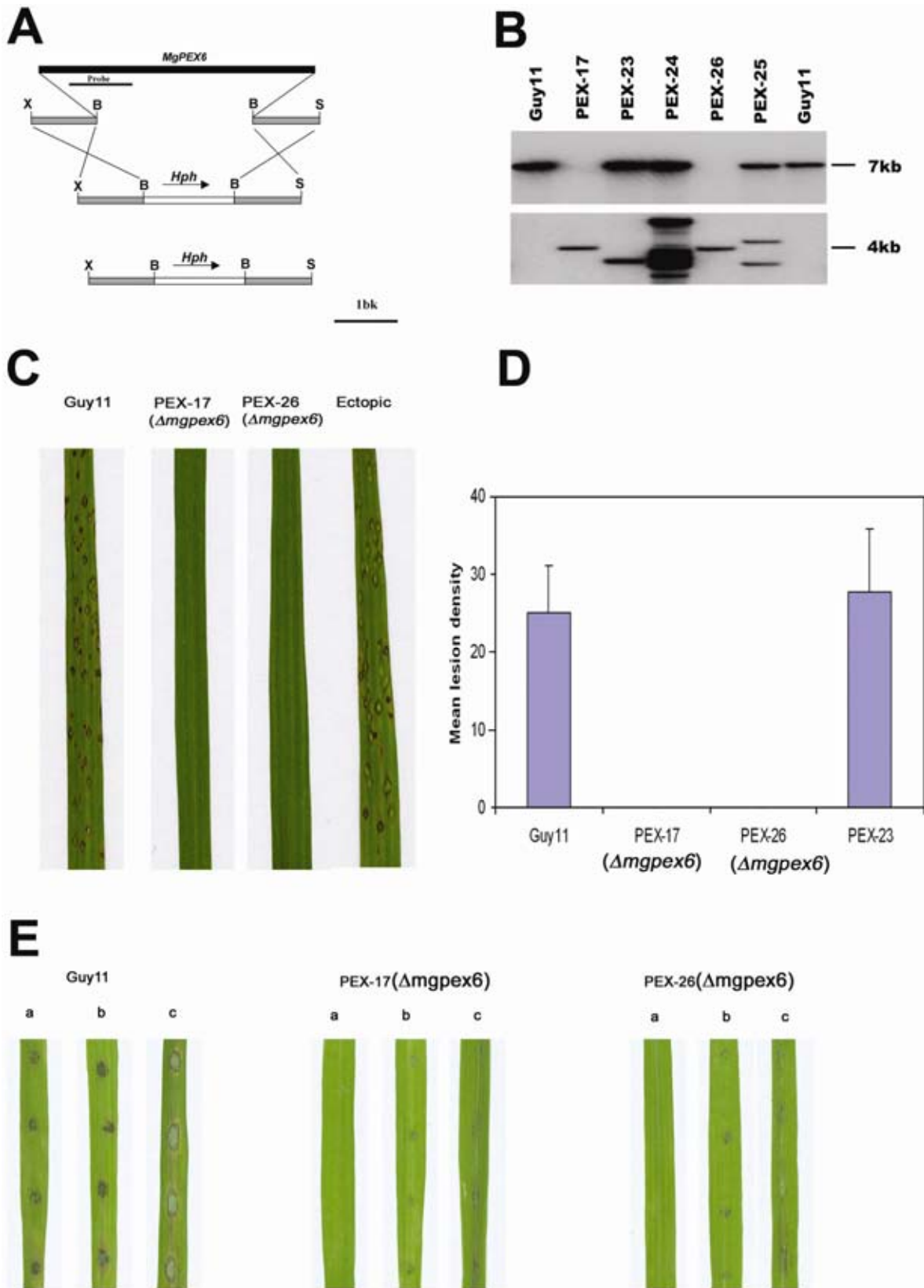


**Fig. 5.** *MgPEX6* gene is necessary for rice blast disease **A**, The *MgPEX6* gene replacement vector was constructed by amplifying two fragments flanking the *MgPEX6* locus and ligating these to the 1.4-kb *Hph* cassette. Restriction enzyme sites are: X, *Xho*I; B, *Bam*HI; S, *Spe*I. All restriction sites were introduced during the cloning process. **B**, DNA gel blot analysis of Guy11, two  $\Delta mgpe x6::Hph$  mutants (PEX-17 and PEX-26), and ectopic transformants PEX-23, PEX-24, and PEX-25. Genomic DNA was digested with *Kpn*I and probed with a 1-kb polymerase chain reaction product which amplified with the primers P-7F and P-8R (top) and *Hph* cassette (bottom). **C**, Leaves of 14-day-old rice seedlings of cv. CO-39 were sprayed with conidia of Guy11, PEX-17, PEX-26, and ectopic transformant PEX-23 at a concentration  $1 \times 10^4$  conidia  $ml^{-1}$ . **D**, Bar chart showing the results of quantitative analysis of rice infection assays. Mean lesion density values recorded from 5-cm sections from 15 of the most infected leaves. Error bars represent the standard deviation. **E**, Rice leaf segments were inoculated with 10- $\mu$ l conidial droplets of Guy11 and  $\Delta mgpe x6::Hph$  mutants: PEX-17 and PEX-26 at a concentration of  $1 \times 10^4$  conidia  $ml^{-1}$ ; a = unwounded leaf, b = addition of 2.5% glucose to conidial suspension, and c = abraded leaf.

RNA gel blot experiments showed that *MgPEX6* is highly expressed in conidia and in the presence of olive oil as a sole carbon source (Fig. 6A). To examine spatial analysis of *MgPEX6* expression, a C-terminal fusion of the *sGFP* allele was made to the protein-coding sequence of *MgPEX6* downstream of a 1.5-kb fragment of its native promoter. The *MgPEX6:sGFP* plasmid was introduced into *Δmgpex6* mutant PEX-26 and transformants with a single integration of the plasmid were selected. Two independent transformants, PEX-G-9 and PEX-G-10, showed complementation of the *Δmgpex6* mutant phenotypes (data not shown) and were used to investigate gene expression and MgPex6 localization patterns. Conidia from PEX-G-9 exhibited higher levels of GFP fluorescence than vegetative hyphae and MgPex6-GFP was mainly cytosolic in both conidia and mycelium (Fig. 6B). This is consistent with a role in assembly of peroxisomes throughout the cell.

Peroxisome matrix proteins usually contain PTSs for correct import to the organelle. To investigate the import of peroxisome matrix proteins in *Δmgpex6* mutants, we transformed plasmid pMLH21-bar (Maggio-Hall and Keller 2004), which carries the PTS1 targeting sequence from *A. nidulans foxA* fused to the C-terminus of the RFP, into Guy11 and *Δmgpex6* mutant PEX-26. Single-copy plasmid insert transformants were identified by DNA gel blot and investigated by epifluorescence microscopy. When *RFP-foxA-PTS* was expressed in Guy11, abundant punctate fluorescence was observed in the transformants, consistent with peroxisomal import of *RFP-foxA-PTS*, (Fig. 6C). In contrast, when *RFP-foxA-PTS* was expressed in the *Δmgpex6* mutant PEX-26, diffuse fluorescence was observed throughout the cytoplasm (Fig. 6D). When *MgPEX6:sGFP* was introduced into the *Δmgpex6* mutant PEX-R-29, this restored the peroxisomal localization of *RFP-foxA-PTS* (Fig. 6E). When considered together, these results indicate that *Δmgpex6* mutants are defective in import of peroxisome matrix proteins containing the PTS1 motif and that MgPex6 of *M. grisea* is necessary for peroxisome biogenesis.

#### ***MFPI* and *MgPEX6* are preferentially expressed during appressorium development of *M. grisea*.**

To investigate temporal regulation of peroxisomal fatty acid  $\beta$ -oxidation during plant infection by *M. grisea*, *MFPI:sGFP*- and *MgPEX6:sGFP*-expressing transformants were selected and conidia from each strain were germinated on a hydrophobic plastic surface that induces infection structure formation (Talbot et al. 1993). *MFPI:sGFP* expression was observed in conidia and remained at a similar level during germ tube emergence and elongation. However, maximal expression of *MFPI:sGFP* was observed in appressoria between 24 and 48 h after spore germination, during turgor generation (Fig. 7). Expression of *MgPEX6:sGFP* also was observed in conidia and during germ tube elongation and appressorium maturation. At 24 h after spore germination, *MgPEX6:sGFP* fluorescence was observable only in the appressorium (Fig. 7). The expression of both *MFPI:sGFP* and *MgPEX6:sGFP* was followed throughout the infection process of plant cuticles and less fluorescence was observed in invasive hyphae after plant infection (data not shown). Therefore, gene expression leading to peroxisomal biogenesis and fatty acid  $\beta$ -oxidation occurs predominantly during the prepenetration stage of development of *M. grisea*.

#### **Plant cuticle penetration by *M. grisea* requires *MFPI* and *MgPEX6*.**

To determine why *Δmfpl* and *Δmgpex6* mutants are unable to cause rice blast disease, the ability of these mutants to penetrate intact plant epidermal cells was determined (Chida and Sisler 1987). Successful production of penetration hyphae from the base of appressoria of *Δmfpl* mutants was found to occur 51.40  $\pm$

25.26% of the time in MBO-7, compared with 93.60  $\pm$  2.07% successful penetrations by Guy11 (Supplementary Figure 5). In *Δmgpex6* mutants, which are unable to cause rice blast symptoms, formation of penetration hyphae and rupture of the plant epidermis was significantly decreased from 93.60  $\pm$  2.07% successful penetrations by Guy11 to only 3.40  $\pm$  3.65% successful penetrations in *Δmgpex6* mutant PEX-26. Appressorium-mediated penetration requires very high internal turgor to facilitate generation of the mechanical force to breach the rice leaf cuticle. Appressorium turgor can be measured using an incipient cytorrhysis assay, which uses hyperosmotic concentrations of a solute to collapse appressoria, thereby allowing estimation of their internal solute concentration and turgor (de Jong et al. 1997; Howard et al. 1991). To carry out this assay, appressoria were allowed to form on a hydrophobic plastic surface and then incubated in glycerol solutions of varying concentration. No significant decrease in appressorium turgor was observed in *Δmfpl* mutants (data not shown). The appressoria formed by *Δmgpex6* did, however, show plasmolysis rather than cytorrhysis by high exogenous glycerol solutions (data not shown) consistent with permeability of the appressorial wall to glycerol and, therefore, depletion of appressorium melanin (de Jong et al. 1997; Howard et al. 1991). Therefore, ultrastructural analysis was carried out to investigate the melanization of appressoria in both mutants. Melanin is deposited as a conspicuous, partially electron-dense layer in appressoria in *M. grisea* Guy11 (Fig. 8). The melanin layer in appressoria of *Δmfpl* mutants was thinner than that of Guy11, and no obvious melanized layer was observed in appressoria of *Δmgpex6* mutants (Fig. 8). We conclude that the activities of both *Mfpl* and *MgPex6* are required for elaboration of fully functional appressoria by *M. grisea*.

#### **Mobilization and degradation of lipid droplets is delayed in *Δmfpl* and *Δmgpex6* mutants of *M. grisea*.**

Appressorium development in *M. grisea* is accompanied by rapid translocation of lipid droplets from the conidium to the nascent appressorium, a process regulated by the Pmk1 MAP kinase signaling pathway (Thines et al. 2000). To determine if impairment of peroxisome biogenesis and fatty acid  $\beta$ -oxidation affected lipid body mobilization, Nile red staining of intracellular lipid stores was carried out during appressorium morphogenesis of *Δmfpl* and *Δmgpex6* mutants. In the wild-type Guy11, lipid droplets were transported to the incipient appressorium within 6 h (Fig. 9). During appressorium maturation, large lipid deposits were observed within appressoria, where they coalesced and were taken up into vacuoles (Weber et al. 2001). Lipid degradation then occurred rapidly during appressorium maturation (12 h), and fully melanized appressoria formed 24 to 48 h after germination were almost entirely devoid of lipid droplets. In both *Δmfpl* and *Δmgpex6* mutants, similar numerous lipid droplets were seen in ungerminated conidia (0 h) and germ tubes (2 h). However, brighter and larger lipid droplets were observed in the mutants during late appressorium formation, particularly in *Δpex6* mutants. Lipid droplet translocation occurred more slowly in both mutants when compared with Guy11 and became more evenly distributed throughout the conidium and germ tube. Even after 48 h, some undegraded lipid droplets remained in the conidium, germ tube, and appressorium (Fig. 9), indicating that impairment of peroxisomal function prevents appressorium lipolysis from taking place and renders the appressorium incapable of penetrating the host cuticle.

## **DISCUSSION**

The rice blast fungus produces a specialized infection structure that is used to penetrate the rice plant cuticle using mechanical force. This structure, the appressorium, develops

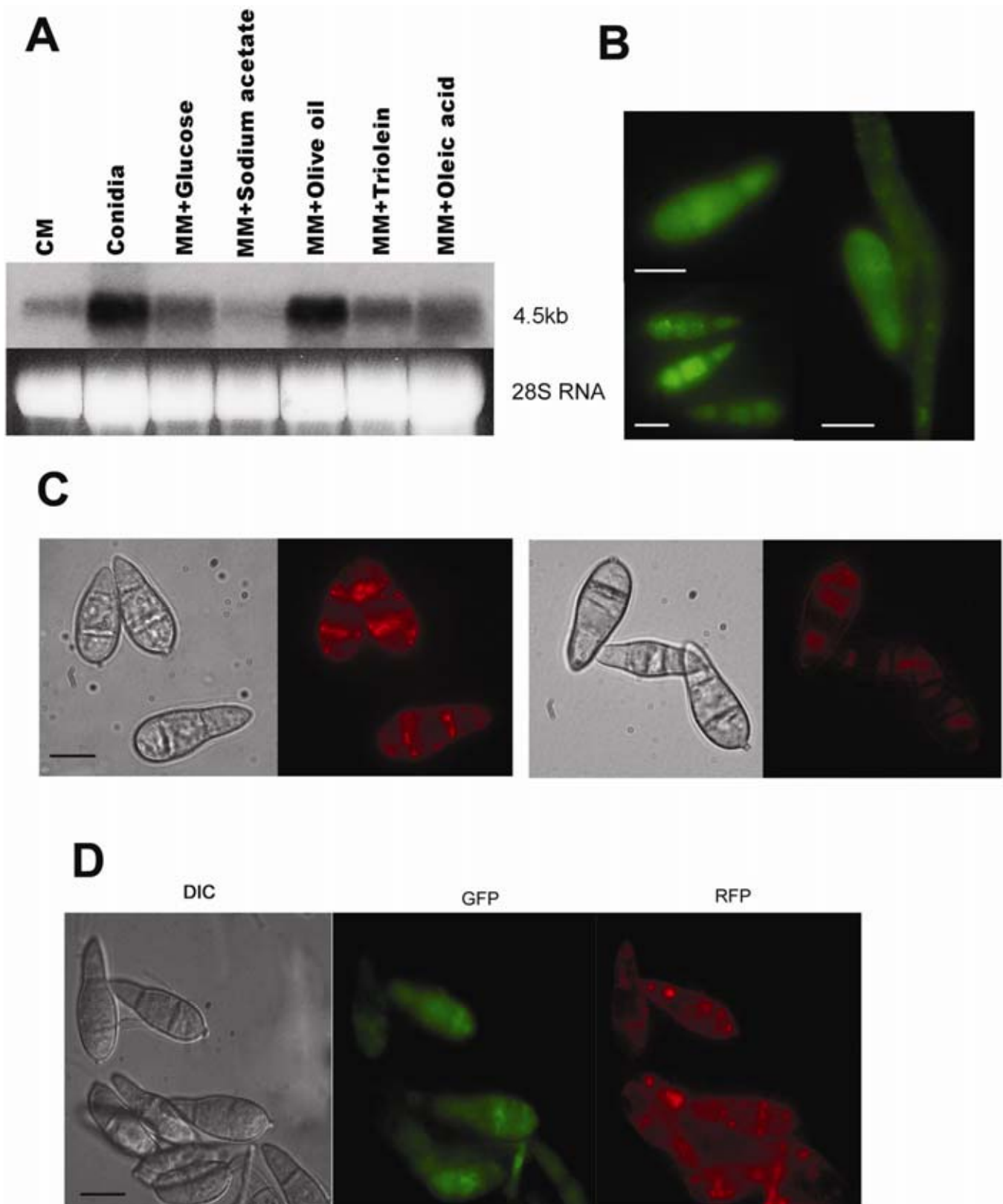


**Fig. 6.** Expression of *MgPEX6* and subcellular localization of MgPex6-green fluorescent protein (GFP) of *Magnaporthe grisea*. **A**, RNA gel blot analysis of *MgPEX6* expression. Total RNA was extracted from *M. grisea* mycelium grown in complete medium (CM), or minimal medium with glucose, sodium acetate, olive oil, triolein, and oleic acid as sole carbon source, or from fungal spores. **B**, MgPex6-GFP cytosolic localization in conidia and hyphae of transformant PEX-G-9. **C**, MgPex6-dependent peroxisomal localization of the red fluorescent protein (RFP)-peroxisomal targeting signal 1 (PTS1) fusion protein. The RFP-foxA gene fusion, which carries a C-terminal type I peroxisomal targeting sequence, was transformed in Guy11 to create GY-4. RFP expression was observed in conidia by epifluorescence microscopy. The same construct was transformed into a *Δmgpex6* mutant PEX-R-29. **D**, Intracellular localization of the MgPEX6 and RFP-PTS1 fusion protein in PEX-R-G-29-1. Bar for all frames = 10 μm.

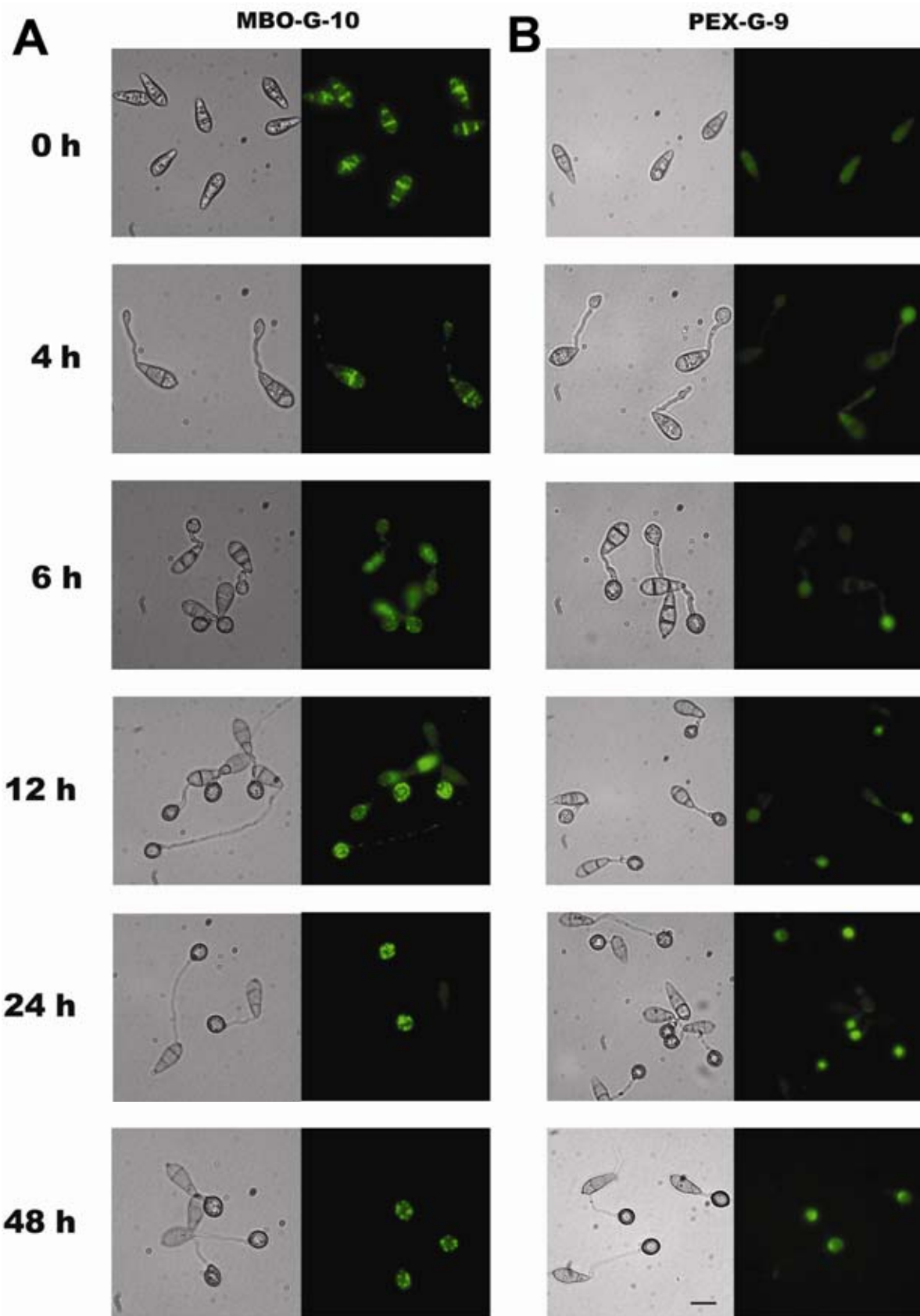


**Fig. 7.** *Magnaporthe grisea* *MFP1* and *MgPEX6* are highly expressed during infection-related development **A**, Expression of *M. grisea* Mfp1-green fluorescent protein (GFP) during conidial germination and appressorium development. Strain MBO-G-10 is a *MFP1::sGFP::ILV1* transformant of  $\Delta mfp1$  mutant MBO-7, which complemented all mutant phenotypes. Conidia were allowed to germinate on glass coverslips, forming germ tubes within 4 h and nascent, dome-shaped appressoria by 6 to 8 h, which developed turgor and became melanized by 24 h. Mfp-GFP-containing peroxisomes moved into appressoria together with cytoplasm during conidial collapse and were visible during turgor generation. **B**, Strain PEX-G-9 is a *MgPEX6::sGFP::ilv1* transformant of  $\Delta mgpex6$  mutant, PEX-26, and was used to analyze the expression of *M. grisea* MgPex6-GFP during conidial germination and appressorium development. The MgPex6 peroxin was localized predominantly in appressoria during their development and maturation. Bar for all frames = 10  $\mu$ m.

soon after the fungus lands on the rice leaf surface and its development is the result of a morphogenetic program that is linked to mitotic cell division in the fungal germ tube and autophagic cell death of the fungal conidium (Veneault-Fourrey et al. 2006). The contents of the fungal spore are translocated to the dome-shaped appressorium in order to generate the enormous cellular turgor required for cuticle penetration. Previous biochemical analysis has shown that the activity of triacylglycerol lipases is induced during appressorium maturation and that lipid bodies are rapidly mobilized from the conidium to the appressorium, where they are degraded prior to plant infection (Thines et al. 2000). This study set out to investigate the role that lipid metabolism might play in plant infection by a pathogenic fungus.

Analysis of the genome sequence of *M. grisea* (Dean et al. 2005) showed that the fungus has at least 7 genes that are predicted to encode intracellular triacylglycerol lipases and 21 genes that are predicted to encode extracellular lipases or esterases (Tables 1 and 2). We obtained eight different lipase mutants and one double mutant by targeted gene deletion of *M. grisea*. However, rice leaf infection assays showed that all of these mutants had an ability to cause rice blast disease similar to that of wild-type strain Guy11. These results suggested that intracellular lipases of *M. grisea* may have overlapping functions and, therefore, contribute to the high levels of appressorium triacylglycerol lipase activity found in appressoria (Thines et al. 2000) in a more complex manner than can be tested readily by individual gene functional analysis. It is likely that gene silencing of the entire repertoire of triacylglycerol lipase genes by utilization of RNA interference, which has been shown to be possible in *M. grisea* (Kadotani et al. 2004), may provide the most useful strategy for determining the mechanism of appressorial lipolysis in the rice blast fungus. One lipase-encoding gene, *HDL2*, proved to be recalcitrant to gene replacement; therefore, it is also possible that this lipase is essential for cell viability or plays a critical role in appressorium function. Gene silencing offers the best strategy to investigate such a possibility.

A direct consequence of intracellular lipolysis, which accompanies appressorium maturation, is likely to be the generation of fatty acids, which are metabolized by  $\beta$ -oxidation. The genome sequence of *M. grisea* indicates that both mitochondrial and peroxisomal  $\beta$ -oxidation are likely to take place in the fungus, because the fungus possesses both mitochondrial and peroxisomal forms of acyl-CoA dehydrogenase, which catalyses the first step in  $\beta$ -oxidation, and also possesses predicted mitochondrially lo-

calized short-chain enoyl-CoA hydratase and  $\Delta 3,\tau\Delta$  2-enoyl-CoA isomerase enzymes. This is consistent with recent studies in *A. nidulans* (Maggio-Hall and Keller 2004), in which the growth of a peroxisomal  $\beta$ -oxidation mutant lacking the FoxA-encoded multifunctional protein was shown to be blocked or partially impaired on very long or long-chain fatty acids, but was not affected on short-chain fatty acids. In contrast, growth on short-chain fatty acids instead required mitochondrial  $\beta$ -oxidation and did not occur in an enoyl coA hydratase mutant (Maggio-Hall and Keller 2004). The *M. grisea* genome sequence also showed a large inventory of acyl CoA dehydrogenases, providing evidence that the fungus can utilize a wide range of fatty acids as substrate, including branched-chain fatty acids. In contrast, in spite of the apparent presence of mitochondrial  $\beta$ -oxidation, *M. grisea* is unable to grow effectively on short-chain fatty acids. The fungus was, for example, unable to grow on the six-carbon fatty acid hexanoic acid in either the presence or absence of Mfp1 (data not shown). The presence of acyl CoA dehydrogenases also is consistent with studies in the related Sordariomycete fungus *N. crassa*, in which  $\beta$ -oxidation has been shown to take place in a discrete catalase-free compartment termed a glyoxysome. Here, the initial reaction in each round of  $\beta$ -oxidation is catalyzed by acyl-CoA dehydrogenase (Thieringer and Kunau 1991).

To investigate the role of fatty acid  $\beta$ -oxidation in *M. grisea*, we identified and characterized the *MFPI* gene encoding the multifunctional protein in *M. grisea*, which catalyses the second and third steps of fatty acid  $\beta$ -oxidation. Mutants lacking this gene were unable to use lipids or fatty acids as a sole carbon source and were attenuated in virulence. Although the Mfp1 amino acid sequence analysis did not show obvious peroxisomal targeting sequences, the expression of an Mfp1-GFP gene fusion showed that Mfp1 is localized in peroxisomes, colocalizing with a RFP-foxA gene fusion (Maggio-Hall and Keller 2004) that contains a type I peroxisome targeting sequence. To date, two targeting sequences for peroxisomal matrix proteins have been identified. The most abundant is the PTS type I (PTS1), which consists of a conserved tripeptide at the extreme C-terminus of the protein and a less-conserved upstream region. The consensus sequence of the C-terminal tripeptide is S/A-K/R-L/M, but not all variations are functional in all species. The second PTS (PTS2) is located close to the N-terminus and defined by the less-conserved consensus sequence R-L/I-X5HL (Reumann 2004). Given the absence of an obvious peroxisomal targeting sequence in Mfp1 and its appar-

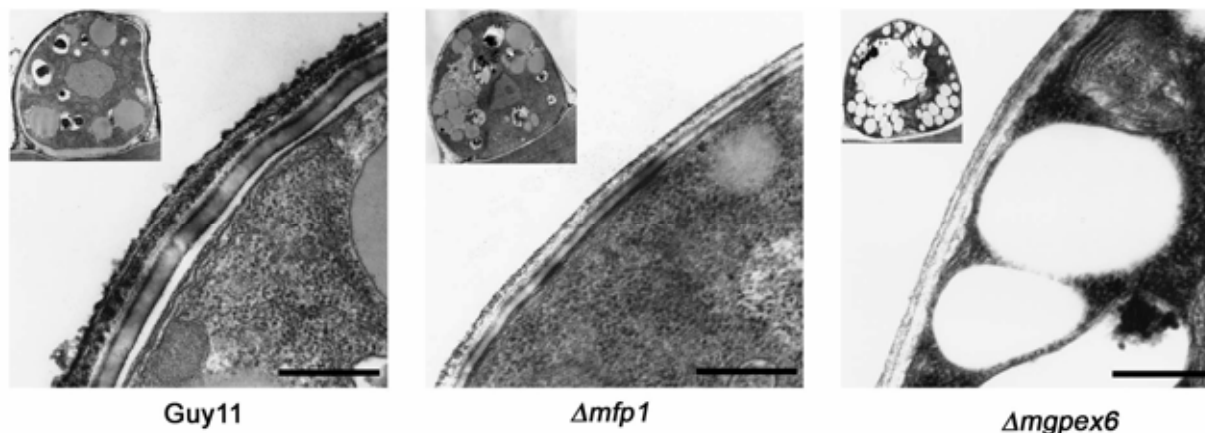


**Fig. 8.** Ultrastructural analysis of the appressorium cell wall of *Magnaporthe grisea*  $\Delta mfp1$  and  $\Delta mgpex6$  mutants. Appressoria were allowed to form on sterile onion epidermis for 24 h and ultrathin sections were processed for transmission electron microscopy. Transverse sections to show detail of the appressorium cell wall are shown. The melanin layer in the appressorium cell wall is indicated with an arrow. The whole appressorium from each transverse section is shown in the panel inset. Bar = 200 nm.

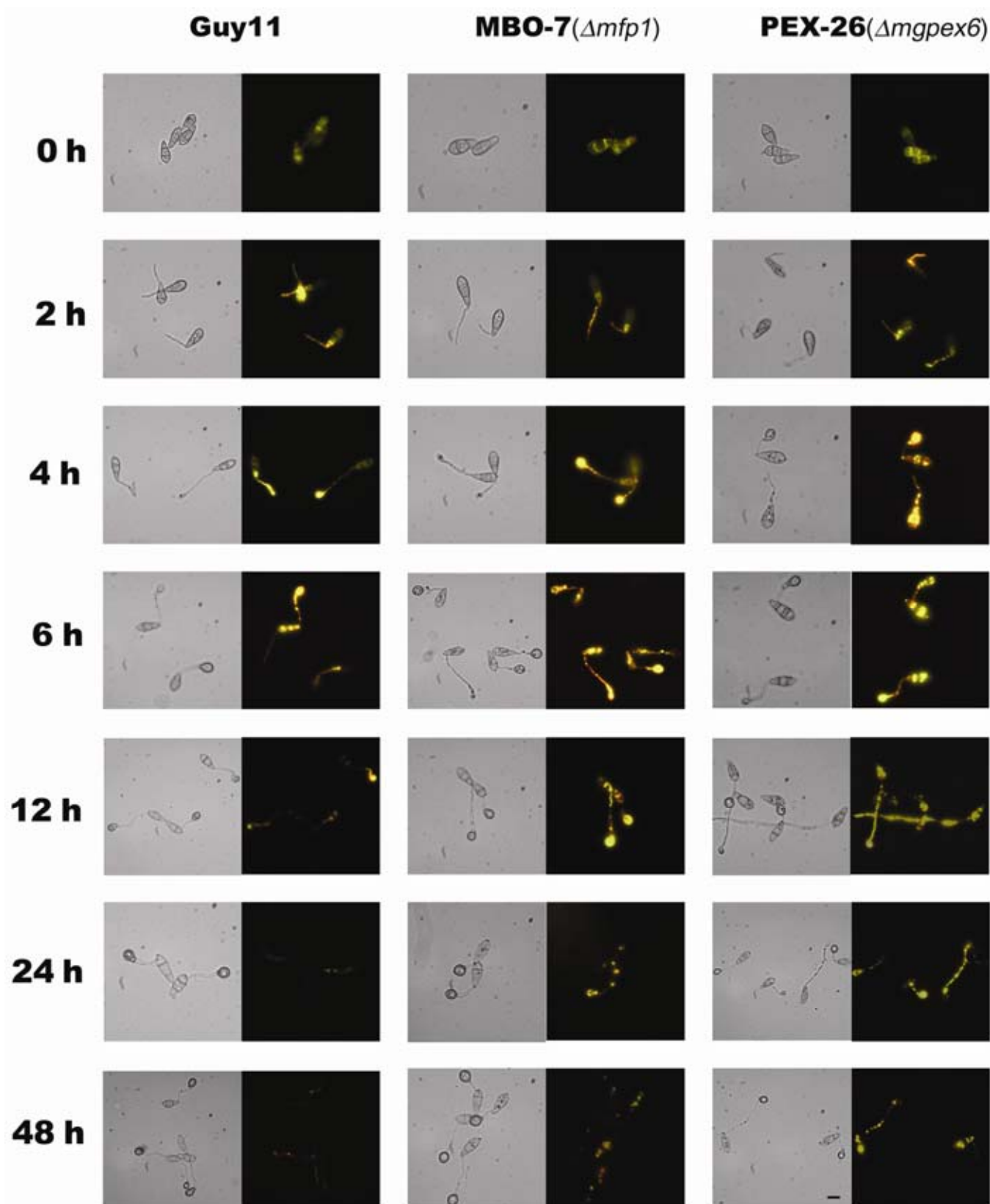


**Fig. 9.** Lipid body movement of *Magnaporthe grisea* Guy11,  $\Delta mfp1$ , and  $\Delta mgpex6$  mutants during appressorium morphogenesis. Conidia of *M. grisea* Guy11, MBO-7 ( $\Delta mfp1$ ), and PEX-26 ( $\Delta mgpex6$ ) were incubated in water droplets on glass coverslips and allowed to form appressoria for 48 h. Samples were removed at 0, 2, 4, 6, 12, 24, and 48 h and stained with Nile red to show the presence of lipid bodies by epifluorescence microscopy. Lipid bodies of Guy11 migrated to the tips of germ tubes and young appressoria and disappeared during the maturation of appressoria. The  $\Delta mfp1$  and  $\Delta mgpex6$  mutants showed a delay in lipid mobilization and degradation and, at 24 or 48 h, some lipid drops were still present in germ tubes and appressoria. Bar for all frames = 10  $\mu$ m.

ent localization to the peroxisomal compartment, it seems likely that further targeting motifs, or alternate mechanisms for transport of proteins into peroxisomes, must exist in *M. grisea*.

Plant infection tests showed Mfp1 to be a significant determinant of rice blast disease. Mutants lacking Mfp1 were dramatically reduced in their ability to infect rice leaves and bring about disease symptoms. This was due to a defect in appressorium function that prevented the initial traversal of the host plant cuticle. Surprisingly, the turgor of the mutant was not significantly reduced, suggesting that the solute, glycerol, is not likely to be derived from the degradation of fatty acids in *M. grisea*. The virulence phenotype of Mfp1 mutants provided evidence that peroxisomal  $\beta$ -oxidation is a critical component of appressorium physiology and is consistent with recent studies that have shown that carnitine acetyl transferase—which catalyzes the traversal of acetyl CoA across the peroxisomal membrane—is necessary for rice blast disease (Bhambra et al. 2006; Ramos-Pamplona and Naqvi 2006). The Pth2-encoded carnitine acetyl transferase initially was identified in a genetic screen for pathogenicity mutants (Sweigard et al. 1998), is peroxisomally located, and is necessary for efficient lipid breakdown in the appressorium. Taken together, these studies (Bhambra et al. 2006; Ramos-Pamplona and Naqvi 2006) and the current report provide evidence that generation of acetyl CoA via fatty acid  $\beta$ -oxidation is a prerequisite for appressorium-mediated plant infection. This also is consistent with observations in the anthracnose fungus, *C. lagenarium*, which also uses melanin-pigmented appressoria to infect host plants, where peroxisome function has been shown to be necessary for infection (Kimura et al. 2001). The fact that fatty acid  $\beta$ -oxidation occurs within peroxisomes during appressorium maturation prompted us to test the effect of preventing peroxisomal biogenesis in *M. grisea* on its ability to cause disease.

Peroxisomes are single-membrane-bound organelles possessing multiple metabolic functions, including fatty acid  $\beta$ -oxidation, glyoxylate metabolism, and metabolism of reactive oxygen species. Genetic and proteomic approaches have led to the identification of 32 proteins, collectively called peroxins, which are required for the biogenesis of peroxisomes (Heiland and Erdmann 2005; Wanders and Waterman 2004). Some peroxins are responsible for the division and inheritance of peroxisomes, although most have been implicated in the topogenesis of peroxisomal proteins. Peroxisomal membrane and matrix proteins are synthesized on free ribosomes in the cytosol and then imported post-translationally into preexisting peroxisomes (Lazarow and Fujiki 1985), which implies that their synthesis and import are sequential rather than simultaneous processes (Wanders and Waterman 2004).

To study the role of peroxisome function in *M. grisea*, we identified and characterized the *PEX6* gene. The peroxin Pex6 is a member of the large family of AAA proteins (ATPase) associated with a wide range of cellular activities. The AAA domain consists of 220 to 230 aa and contains two motifs named Walker A and B which bind and hydrolyze ATP, respectively. The ATPase activity of Pex6 recently has been shown to be required for the ATP-dependent dislocation of the PTS1 receptor from the peroxisomal membrane to the cytosol (Platta et al. 2005). In this study, we found that, in *M. grisea*, the import of PTS1-containing peroxisomal matrix proteins was impaired in *Apex6* mutants. Therefore, Pex6 is likely to be required for matrix protein import during peroxisomal biogenesis in *M. grisea*.

### **The role of peroxisomal fatty acid $\beta$ -oxidation in plant infection.**

The absence of peroxisome biogenesis in *M. grisea* appressoria caused significant defects in appressorium function and a complete loss in pathogenicity. The *Apex6* mutants formed

smaller, often misshapen, appressoria compared with the isogenic wild-type strain Guy11, and ultrastructural analysis showed that these mutants lacked the melanin layer necessary for turgor generation (Howard and Valent 1996; Howard et al. 1991). However, the loss of pathogenesis was not solely attributable to the lack of appressorium function because wounded seedlings inoculated with *Apex6* mutants did not develop rice blast symptoms or support fungal growth. Therefore, in spite of the high level of expression of Pex6 during the prepenetration stage of development, peroxisome function is necessary not only for initial plant infection but also for tissue colonization and proliferation by the fungus. Comparative analysis of both *Amfp1* and *Apex6* mutants showed that both gene functions are necessary for lipid body degradation within developing appressoria, demonstrating that, although the initial degradation of triacylglycerol in infection cells is likely to be a consequence of the orchestrated activity of a number of individual triacylglycerol lipases, the subsequent processing of the liberating fatty acid moieties occurs predominantly through peroxisomal  $\beta$ -oxidation. The resulting acetyl CoA is available for dihydroxynaphthalene melanin biosynthetic pathways and also for processing via the glyoxylate cycle to fuel fungal cell wall biosynthesis during plant infection (Bhambra et al. 2006; Ramos-Pamplona and Naqvi 2006; Wang et al. 2003). The complete absence of pathogenicity in *Apex6* mutants, coupled with our observation of significant proliferation of peroxisomes during appressorium maturation (Fig. 7), suggests that peroxisome biogenesis is developmentally regulated and also might act as a checkpoint for further maturation of the appressorium. The role of *PEX6* in pathogenesis of *M. grisea* also has been discovered independently during analysis of carnitine metabolism in the fungus (Ramos-Pamplona and Naqvi 2006), and the mutant phenotypes associated with appressorium function that were observed are consistent with this study. The role of Pex6 in conidial viability and the necessity of peroxisomal function for invasive growth of the fungus in rice leaves, however, provide evidence for a much more fundamental role in fungal development during pathogenesis that might provide an effective target for disease intervention. It is clear from our observations that *Apex6* mutants retain the capacity to form polarized infection hyphae during plant infection, because colonization of onion epidermal layers can still take place, albeit at reduced levels. However, the traversal of intact rice leaves is severely inhibited, as is the subsequent development of the fungus in plant tissue, perhaps highlighting the significance of peroxisomal fatty acid metabolism and acetyl CoA generation to a range of other biochemical pathways such as secondary metabolism, melanin production, and cell wall biosynthesis (Bhambra et al. 2006).

Recently, it has become clear that appressorium formation by the rice blast fungus is a consequence of a developmental program that links cell cycle progression with programmed autophagic cell death of the three-celled fungal spore and recycling of its contents to the single-celled appressorium, prior to plant infection (Veneault-Fourrey et al. 2006). Blocking autophagic cell death prevents plant infection, demonstrating that translocation and reutilization of the spore contents in the appressorium is key to its ability to breach the cuticle and enter rice tissue (Veneault-Fourrey et al. 2006). Here, we have shown that peroxisomal metabolism is a key component of this tissue remodeling process and is essential both for appressorium function and subsequent proliferation of the fungus in rice leaves. The next challenge will be to determine how peroxisomal biogenesis is coupled to the cell cycle-controlled development of appressoria and the regulation of autophagy and how these processes collectively allow plant infection to proceed.

## MATERIALS AND METHODS

### Fungal strains, growth conditions, and DNA analysis.

*M. grisea* maintenance, media composition, nucleic acid extraction, and fungal transformation were all as described previously (Talbot et al. 1993). Minimal medium was supplemented with glucose at 10 g liter<sup>-1</sup> as sole carbon source or an equivalent amount of alternative carbon sources (acetate, oleic acid, or triolein). Molecular biology methods were performed using standard procedures (Sambrook et al. 1989).

### Construction of targeted gene replacement vectors.

Methods describing the construction of gene replacement vectors for generation of *Atgl1-1*, *Atgl1-2*, *Atgl2*, *Atgl3-1*, *Atgl3-2*, *Ahd11*, *Ahd13*, and *Avt11* and the double mutant *Atgl3-1 Atgl3-2* are provided in the online Supplementary Methods and Supplementary Table 1. For construction of the *MFPI* gene replacement vector, a 5.35-kb fragment spanning the *MFPI* locus was amplified with primers M-1F and M-2F (Supplementary Table 2 lists all primer sequences), and a 2.3-kb *ClaI* and *Bsu36I* fragment containing the majority of the *MFPI* ORF was removed and replaced with the 1.4-kb *Hph* gene cassette, which encodes hygromycin phosphotransferase under the control of the *A. nidulans* TrpC promoter (Carroll et al. 1994). The resulting plasmid was digested with *BamHI* and *SpeI* to liberate a linear gene disruption cassette to transform *M. grisea* Guy11. For replacement of *MgPEX6*, 1-kb flanking sequences on either side of the gene locus were amplified using primers P1-F, P2-R, P3-F, and P4-R and cloned sequentially into pGEM-T (Promega Corp., Madison, WI, U.S.A.), leaving a single *BamHI* site for insertion of the *Hph* gene cassette. The resulting construct allows removal of a 4.3-kb fragment containing the whole *PEX6* coding region and was used to transform *M. grisea* Guy11.

### Gene expression and localization studies.

Full-length cDNAs of *MFPI* and *MgPEX* were obtained by RACE polymerase chain reaction (PCR) amplification (BD Biosciences, San Jose, CA, U.S.A.) and were completely sequenced to confirm the positions of introns and translational start and end sites. The C-terminal GFP tagging vector, *MFPI-sGFP*, was constructed by amplification of the 3.1-kb *MFPI* gene-coding sequence and a 1.5-kb promoter fragment using primers M-3F and M-4R. The M-4R primer adds a *SpeI* site at the last codon of *MFPI*. The 4.6-kb fragment was cloned into pCB1532, which contains the *ILVI* gene conferring resistance to sulfonyleurea (Sweigard et al. 1997) to give pMBO-G. The *sGFP* allele (Chiu et al. 1996) carrying the *A. nidulans trpC* terminator (Punt et al. 1987) was amplified by PCR using primers GFP-Spe-F and GFP-EcoR-R, digested with *SpeI* and *EcoRI*, and ligated into pMBO-G to create *MFPI-sGFP*. The resulting plasmid, *MFPI-sGFP*, was checked by DNA sequencing to confirm in-frame fusion and used to transform into *Amfp1* mutant MBO-7. Transformants carrying a single insertion were selected and complementation of the *Amfp1* mutant phenotypes checked prior to epifluorescence microscopy.

The *MgPEX6-sGFP* plasmid was made by amplifying a 5.9-kb fragment of *MgPEX6* containing 1.57 kb of upstream promoter sequence and the entire protein-coding sequence, using primer P-5F and P-6R. Primer P-6R added an *XhoI* site at the last codon of *MgPEX6*. The amplicon was cloned into pCB1532 to generate pPEX-G. The *sGFP* allele was amplified by PCR using primers GFP-Xho-F and GFP-Xho-R, digested with *XhoI*, and ligated into pPEX-G to create *MgPEX6-sGFP*. The resulting plasmid was checked by DNA sequencing to confirm in-frame fusion and used to transform the *Amgpex6* mutant PEX-26. Transformants carrying a single insertion were selected using epifluorescence microscopy.

The RFP-foxA expression vector was based on plasmid pLMH21 (Maggio-Hall and Keller 2004). The plasmid was digested with *EcoRI* to remove the *argB* gene and replace this with the *bar* selectable marker which confers resistance to bialaphos (Sweigard et al. 1997). The resulting plasmid was transformed into Guy11, *MFPI:sGFP* transformant MBO-G-10, and *Apex6* mutant PEX-26. Transformants carrying a single insertion were detected using epifluorescence microscopy with a Zeiss Axioskop 2 fluorescence microscope (Carl Zeiss, Jena, Germany).

### Measurement of lipid mobilization.

Lipid droplets in the germinating *M. grisea* conidia and appressoria of *Amfp1* and *Amgpex6* gene replacement mutants and Guy11 were visualized by staining with a Nile Red solution (Thines et al. 2000; Weber et al. 1999) consisting of 50 mM Tris-maleate buffer, pH 7.5, with polyvinylpyrrolidone at 20 mg ml<sup>-1</sup> and Nile Red Oxazone (9-diethylamino-5H-benzo[ $\alpha$ ]phenoxazine-5-one) at 2.5  $\mu$ g ml<sup>-1</sup> (Sigma-Aldrich, St. Louis). *M. grisea* conidia were obtained by harvesting plate cultures of the fungus grown on complete medium (Talbot et al. 1993) in a cycle of 14 h of light and 10 h of dark at 24°C for 10 days. Conidia were harvested by scraping sporulating cultures with a glass rod in sterile distilled water, followed by centrifugation at 1,000  $\times$  g for 10 min and resuspension in distilled water to a concentration of 1  $\times$  10<sup>4</sup> spores ml<sup>-1</sup>. Conidia were incubated on glass cover slips in a damp chamber at 24°C and observed for appressorium formation and lipid mobilization at intervals. In all cases, suitable material was mounted directly in fresh Nile Red staining solution. Within a few seconds, lipid droplets began to fluoresce when viewed with a microscope with episcopic fluorescence attachment. No fluorescence was observed when Nile Red was omitted from the staining solution.

### Cuticle penetration and plant infection assays.

Penetration of onion epidermal strips was assessed by the procedure of Chida and Sisler (1987). *M. grisea* conidia were harvested from 10-day-old cultures, incubated on strips of onion epidermis, and observed for elaboration of penetration hyphae at 24 and 48 h by microscopy. Rice seedling infections were carried out as described previously (Talbot et al. 1993). Conidial suspensions were diluted in 0.2% gelatin to 1  $\times$  10<sup>4</sup> conidia ml<sup>-1</sup> for rice infections using the dwarf Indica rice cv. CO-39. In the complementation experiments, 1  $\times$  10<sup>5</sup> conidia ml<sup>-1</sup> inoculum was used. Conidia were spray-inoculated using an artist's airbrush onto 14-day-old (two- to three-leaf stage) plants. Rice seedlings were incubated in plastic bags for 24 h to maintain high humidity and then transferred to controlled environment chambers at 24°C and 90% relative humidity with illumination and 14-h light periods. Plants were incubated for 5 days for disease symptom development. A cut-leaf assay was carried out as follows. Rice leaf fragments were cut from 14-day-old CO-39 seedlings and placed on square plastic plates containing 4% agar. Droplets (10  $\mu$ l) of conidial suspensions at 1  $\times$  10<sup>4</sup> conidia ml<sup>-1</sup> were placed carefully on leaf sections and the leaves incubated in a cycle of 14 h of light and 10 h of dark at 24°C for 5 days. Wounded rice leaves were prepared by removing the surface cuticle by abrasion with an emery board.

## ACKNOWLEDGMENTS

This work was supported by a grant to N. J. Talbot from the Biotechnology and Biological Sciences Research Council (BBSRC). The authors gratefully acknowledge useful discussions with M. Ramos-Pamplona and N. Naqvi (Temasek Life Science Laboratory, Singapore), and G. Wakley for help with electron microscopy.

## LITERATURE CITED

- Athenstaedt, K., and Daum, G. 2003. YMR313c/TGL3 encodes a novel triacylglycerol lipase located in lipid particles of *Saccharomyces cerevisiae*. *J. Biol. Chem.* 278: 23317-23323.
- Bhambra, G. K., Wang, Z. Y., Soanes, D. M., Wakley, G. E., and Talbot, N. J. 2006. Peroxisomal carnitine acetyl transferase is required for elaboration of penetration hyphae during plant infection by *Magnaporthe grisea*. *Mol. Microbiol.* 61:46-60.
- Carroll, A. M., Sweigard, J. A., and Valent, B. 1994. Improved vectors for selecting resistance to hygromycin. *Fungal Genet. Newsl.* 41:22.
- Chida, T., and Sisler, H. D. 1987. Restoration of appressorial penetration ability by melanin precursors in *Pyricularia oryzae* treated with anti-penetrants and in melanin-deficient mutants. *J. Pestic. Sci.* 12:49-55.
- Chiu, W. L., Niwa, Y., Zeng, W., Hirano, T., Kobayashi, H., and Sheen, J. 1996. Engineered GFP as a vital reporter in plants. *Curr. Biol.* 6:325-330.
- Dean, R. A. 1997. Signal pathways and appressorium morphogenesis. *Annu. Rev. Phytopathol.* 35:211-234.
- Dean, R. A., Talbot, N. J., Ebbole, D. J., Farman, M. L., Mitchell, T. K., Orbach, M. J., Thon, M., Kulkarni, R., Xu, J. R., Pan, H., Read, N. D., Lee, Y. H., Carbone, I., Brown, D., Oh, Y. Y., Donofrio, N., Jeong, J. S., Soanes, D. M., Djonovic, S., Kolomiets, E., Rehmeyer, C., Li, W., Harding, M., Kim, S., Lebrun, M. H., Bohnert, H., Coughlan, S., Butler, J., Calvo, S., Ma, L. J., Nicol, R., Purcell, S., Nusbaum, C., Galagan, J. E., and Birren, B. W. 2005. The genome sequence of the rice blast fungus *Magnaporthe grisea*. *Nature* 434:980-986.
- de Jong, J. C., McCormack, B. J., Smirnov, N., and Talbot, N. J. 1997. Glycerol generates turgor in rice blast. *Nature* 389:244-245.
- Ecker, J. H., and Erdmann, R. 2003. Peroxisome biogenesis. *Rev. Physiol. Biochem. Pharmacol.* 147:75-121.
- Fickers, P., Fudalej, F., Le Dall, M. T., Casaregola, S., Gaillardin, C., Thonart, P., and Nicaud, J. M. 2005. Identification and characterization of LIP7 and LIP8 genes encoding two extracellular triacylglycerol lyases in the yeast *Yarrowia lipolytica*. *Fungal Genet. Biol.* 42:264-274.
- Hamer, J. E., Howard, R. J., Chumley, F. G., and Valent, B. 1988. A mechanism for surface attachment in spores of a plant pathogenic fungus. *Science* 239:288-290.
- Harbitz, I., Langset, M., Ege, A. G., Hoyheim, B., and Davies, W. 1999. The porcine hormone-sensitive lipase gene: sequence, structure, polymorphisms and linkage mapping. *Anim. Genet.* 30:10-15.
- Heiland, I., and Erdmann, R. 2005. Biogenesis of peroxisomes: Topogenesis of the peroxisomal membrane and matrix proteins. *FEBS (Fed. Eur. Biochem. Soc.) J.* 272:2362-2372.
- Hiltunen, J. K., Mursula, A. M., Rottensteiner, H., Wierenga, R. K., Kastaniotis, A. J., and Gurvitz, A. 2003. The biochemistry of peroxisomal  $\beta$ -oxidation in the yeast *Saccharomyces cerevisiae*. *FEMS (Fed. Eur. Microbiol. Soc.) Microbiol. Rev.* 27:35-64.
- Howard, R. J., and Valent, B. 1996. Breaking and entering—host penetration by the fungal rice blast pathogen *Magnaporthe grisea*. *Annu. Rev. Microbiol.* 50:491-512.
- Howard, R. J., Ferrari, M. A., Roach, D. H., and Money, N. P. 1991. Penetration of hard substrates by a fungus employing enormous turgor pressures. *Proc. Natl. Acad. Sci. U.S.A.* 88:11281-11284.
- Idnurm, A., and Howett, B. J. 2002. Isocitrate lyase is essential for the pathogenicity of the fungus *Leptosphaeria maculans* to canola (*Brassica napus*). *Eukaryotic Cell* 1:719-724.
- Kadotani, N., Nakayashiki, H., Tosa Y., and Mayama S. 2004. One of the two Dicer-like proteins in the filamentous fungi *Magnaporthe oryzae* genome is responsible for hairpin RNA-triggered RNA silencing and related small interfering RNA accumulation. *J. Biol. Chem.* 279:44467-44474.
- Kimura, A., Takano, Y., Furusawa, I., and Okuni, T. 2001. Peroxisomal metabolic function is required for appressorium-mediated plant infection by *Colletotrichum lagenarium*. *Plant Cell* 13:1945-1957.
- Köffel, R., Tiwari, R., Falquet, L., and Schneider, R. 2005. The *Saccharomyces cerevisiae* YLL012/YEH1, YLR020/YEH2, and TGL1 genes encode a novel family of membrane-anchored lipases that are required for sterol ester hydrolysis. *Mol. Cell. Biol.* 25:1655-1668.
- Lazarow, P. B., and Fujiki, Y. 1985. Biogenesis of peroxisomes. *Annu. Rev. Cell Biol.* 1:489-530.
- Lorenz, M. C., and Fink, G. R. 2001. The glyoxylate cycle is required for fungal virulence. *Nature* 412:83-86.
- Maggio-Hall, L. A., and Keller, N. P. 2004. Mitochondrial  $\beta$ -oxidation in *Aspergillus nidulans*. *Mol. Microbiol.* 54:1173-1185.
- Nagao, T., Shimada, Y., Sugihara, A., and Tominaga, Y. 1994. Cloning and nucleotide sequence of cDNA encoding a lipase from *Fusarium heterosporum*. *J. Biochem.* 116:536-540.
- Platta, H. W., Grunau, S., Rosenkranz, K., Girzalsky, W., and Erdmann, R. 2005. Functional role of the AAA peroxins in dislocation of the cycling PTS1 receptor back to the cytosol. *Nat. Cell Biol.* 7:817-822.
- Punt, P. J., Oliver, R. P., Dingemans, M. A., Pouwels, P. H., and Van den Hondel, C. A. M. J. 1987. Transformation of *Aspergillus* based on the Hygromycin-B resistance marker from *Escherichia coli*. *Gene* 56:117-124.
- Ramos-Pamplona, M., and Naqvi, N. I. 2006. Host invasion during rice-blast disease requires carnitine-dependent transport of peroxisomal acetyl-CoA. *Mol. Microbiol.* 61:61-75.
- Reumann, S. 2004. Specification of the peroxisome targeting signals type 1 and type 2 of plant peroxisomes by bioinformatics analyses. *Plant Physiol.* 135:783-800.
- Sambrook, J., Fritsch, E. F., and Maniatis, T. 1989. *Molecular Cloning: A Laboratory Manual*. Cold Spring Harbor Laboratory Press, Cold Spring Harbor, NY, U.S.A.
- Solomon, P. S., Lee, R. C., Wilson, T. C. J., and Oliver, R. P. 2004. Pathogenicity of *Stagonospora nodorum* requires malate synthase. *Mol. Microbiol.* 53:1065-1073.
- Sweigard, J. A., Carroll, A. M., Farrall, L., and Valent, B. 1997. A series of vectors for fungal transformation. *Fungal Genet. Newsl.* 44:52-53.
- Sweigard, J. A., Carroll, A. M., Farrall, L., Chumley, F. G., and Valent, B. 1998. *Magnaporthe grisea* pathogenicity genes obtained through insertional mutagenesis. *Mol. Plant-Microbe Interact.* 11:404-412.
- Talbot, N. J. 2003. On the trail of a cereal killer: exploring the biology of *Magnaporthe grisea*. *Annu. Rev. Microbiol.* 57:177-202.
- Talbot, N. J., Ebbole, D. J., and Hamer, J. E. 1993. Identification and characterisation of *MPG1* a gene involved in pathogenicity from the rice blast fungus *Magnaporthe grisea*. *Plant Cell* 5:1575-1590.
- Thieringer, R., and Kunau, W. H. 1991. The beta-oxidation system in catalase-free microbodies of the filamentous fungus *Neurospora crassa*. Purification of a multifunctional protein possessing 2-enoyl-CoA hydratase, L-3-hydroxyacyl-CoA dehydrogenase, and 3-hydroxyacyl-CoA epimerase activities. *J. Biol. Chem.* 266:13110-13117.
- Thines, E., Weber, R. W. S., and Talbot, N. J. 2000. MAP kinase and protein kinase A-dependent mobilisation of triacylglycerol and glycogen during appressorium turgor generation by *Magnaporthe grisea*. *Plant Cell* 12:1703-1718.
- Van Heusden, G. P., Nebohacova, M., Overbeeke, T. L., and Steensma, H. Y. 1998. The *Saccharomyces cerevisiae* TGL2 gene encodes a protein with lipolytic activity and can complement an *Escherichia coli* diacylglycerol kinase disruptant. *Yeast* 14:225-232.
- van Roermund, C. W. T., Waterham, H. R., Ijlst, L., and Wanders. 2003. Fatty acid metabolism in *Saccharomyces cerevisiae*. *Cell. Mol. Life Sci.* 60:1838-1851.
- Veneault-Fourrey, C., Baroah, M., Egan, M., Wakley, G., and Talbot, N. J. 2006. Autophagic fungal cell death is necessary for infection by the rice blast fungus. *Science* 312:580-583.
- Wanders, R. J. A., and Waterman, H. R. 2004. Peroxisomal disorders I: biochemistry and genetics of peroxisome biogenesis disorder. *Clin. Genet.* 67:107-133.
- Wang, Z. Y., Thornton, C. R., Kershaw, M. J., Debaio, L., and Talbot, N. J. 2003. The glyoxylate cycle is required for correct temporal regulation of virulence by the rice blast fungus *Magnaporthe grisea*. *Mol. Microbiol.* 47:1601-1612.
- Wang, Z. Y., Jenkinson, J. M., Holcombe, L. J., Soanes, D. M., Veneault-Fourrey, C., Bhambra, G. K., and Talbot, N. J. 2005. Molecular biology of appressorium turgor generation by the rice blast fungus *Magnaporthe grisea*. *Biochem. Soc. Trans.* 33:384-388.
- Weber, R. W. S., Wakley, G. E., and Pitt, D. 1999. Histochemical and ultrastructural characterisation of vacuoles and spherosomes as components of the lytic system in hyphae of the fungus *Botrytis cinerea*. *Histochem J.* 31:293-301.
- Weber, R. W. S., Wakley, G. E., Thines, E., and Talbot, N. J. 2001. The vacuole as central element of the lytic system and sink for lipid droplets in maturing appressoria of *Magnaporthe grisea*. *Protoplasma* 216:101-112.
- Yu, J., Hu, S., Wang, J., Wong, G. K. S., Li, S., Liu, B., Deng, Y., Sun, J., Tang, J., Chen, Y., Huang, X., Lin, W., and Chen, Y. 2002. A draft sequence of the rice genome (*Oryza sativa* L. ssp. *indica*). *Science* 296:79-91.
- Zhao, X., Kim, Y., Park, G., and Xu, J. R. 2005. A mitogen-activated protein kinase cascade regulating infection-related morphogenesis in *Magnaporthe grisea*. *Plant Cell* 17:1317-1329.

## AUTHOR-RECOMMENDED INTERNET RESOURCES

- PSORT Prediction website: [psort.ims.u-tokyo.ac.jp/form2.html](http://psort.ims.u-tokyo.ac.jp/form2.html)  
Broad Institute *Magnaporthe grisea* database:  
[www.broad.mit.edu/annotation/fungi/magnaporthe/](http://www.broad.mit.edu/annotation/fungi/magnaporthe/)